Exploring Turbidity Dynamics in the Berendonck Diving Lake

Pedro V. N. R. Teixeira
Supervisors: Maíra Mucci and Miguel Lurling
Thesis number: 2023 M78

April 23, 2024

Contents

Abstract

This thesis explored the dynamics of turbidity in Berendonck Diving Lake, Netherlands, attributed to both anthropogenic and natural factors affecting water clarity. It contributed to the understanding of the current state of Lake Berendonk as part of a larger system analysis, which can be used to select appropriate restoration measures. Additionally, it provided protocols for divers to continuously measure visibility and turbidity. The study investigated the contributions of resuspension, internal nutrient dynamics, and evaluated the efficacy of using coagulants to mitigate high turbidity levels. Incorporating field measurements and laboratory analyses, the research aimed to understand the complexities of aquatic turbidity and internal nutrient cycling. By sampling across different lake zones and depths, the research revealed pronounced variations in water quality indicators such as dissolved oxygen, turbidity, nutrient, and chlorophyll-a concentrations. Sediment analysis highlighted significant internal phosphorus loading (Potential releasable P = 1.86 mg P/g DW sediment), emphasising the role of sediment in nutrient cycling and turbidity. The application of Polyaluminium Chloride (PAC) as a coagulant demonstrated potential in reducing turbidity levels and indicated a promising approach for water clarity restoration, specially for higher levels of turbidity, where 4 mg Al/PAC showed a reduction in turbidity levels.

Introduction

The Netherlands, a nation characterised by its vast waterways and intricate canal systems, has a rich history of water management and land reclamation. Over the centuries, this low-lying country has transformed marshes, swamps, and even sections of the sea into fertile land and artificial lakes. These man-made water bodies, numbering in the thousands, serve a myriad of functions [1]. They range from vast reservoirs used for drinking water supply and flood control, to picturesque urban ponds enhancing the aesthetic appeal of Dutch cities [2]. Some lakes are designed to support vibrant ecosystems, promoting biodiversity with a combination of shallow and deep water zones, while others are oriented towards supporting popular recreational activities such as sailing, swimming, fishing and diving [3]. However, maintaining the ecological balance and water quality in these artificial lakes presents its own set of challenges. Among these challenges are nutrient overloading due to runoff from agricultural lands [4], the introduction of invasive species [5], the proliferation of harmful algal blooms [6] and the rising threat of legacy nutrients from past pollution events [7]. All of these events contribute to the challenge of rising turbidity in aquatic ecosystems [8]. Rising turbidity levels have become a prominent concern, affecting not only the aquatic life but also the clarity of water which has direct implications for various recreational activities [9].

Turbidity in aquatic environments primarily originates from suspended particles. These particles can be categorised into two types: organic and inorganic [10]. The organic fraction mainly includes phytoplankton, which are microscopic autotrophic organisms like cyanobacteria, and dissolved organic materials (DOM) that result from the decomposition of terrestrial plants or other biological residues. These organic compounds not only reduce light penetration but have specific absorption properties. For instance, substances like chlorophyll absorb light mainly at wavelengths around 600 nm and below [10]. A concerning trend is the increase in nutrient pollution, triggering harmful cyanobacterial blooms in many shallow waters, indicative of eutrophication [11, 12]. This process involves excessive nutrients from sources like agricultural runoff and wastewater discharge, which degrade water quality, disrupt aquatic ecosystems, and create oxygen-depleted dead zones [13]. As a result, waters that were once clear have become turbid. These transitions, driven by excess nutrients, negatively impact marine ecosystems and the quality of water for human consumption and recreational activities [14]. On the other hand, inorganic particles comprise materials such as clay like montmorillonite and kaolinite, silt, sand, and various mineral ions. Some, especially clay particles, can alter the light spectrum due to their unique absorption traits. The combined effects of these organic and inorganic particles lead to varying levels of light scattering and absorption, ultimately influencing the water's turbidity and optical properties [10].

Sources of turbidity in aquatic ecosystems include both external and internal factors [15]. External inputs, predominantly from fluvial erosion and inflows, introduce considerable quantities of suspended matter into aquatic ecosystems. This influx of particulates is especially exacerbated during instances of precipitation, where the presence of oversaturated mineral phases, such as calcium carbonate precipitation, can further elevate turbidity levels [16]. In areas subjected to deforestation or extensive cultivation, rainfall events often lead to sediment-laden run-off, amplifying the inherent turbidity of water bodies. Anthropogenic interventions, especially mining, construction endeavours, boating, and diving activities, intensify this sedimentary contribution, introducing a wide array of both organic and inorganic particulates [17]. Beyond direct human influence, natural dynamics within water systems, such as strong currents or wind-induced wave actions, along with the activities of bottom-dwelling species like carp and crayfish, possess the capacity to resuspend settled particles from aquatic substrates. This reshuffles the turbidity profile. The foraging behaviour of carp and the digging and burrowing actions of crayfish contribute significantly [5]. Sediment resuspension has been shown to influence internal nutrient loading and turbidity

in lakes [18]. Resuspension events release nutrients from the sediment back into the water column, enhancing phosphorus availability for algal blooms and contributing to eutrophication. This process not only increases sediment nutrient release but also leads to higher turbidity levels, reducing water clarity and affecting aquatic life. The interplay between resuspension, nutrient release, and turbidity underscores the need for integrated lake management strategies that consider these dynamic processes [19, 20]. All these factors, in tandem, shape the complex interplay of turbidity in aquatic environments.

A comprehensive study by The Netherlands Institute for Ecology (NIOO-KNAW) has highlighted a critical issue affecting smaller water bodies throughout The Netherlands: a stark lack of water clarity due to eutrophic conditions. Alarmingly, 78% of these waters fail to reach acceptable ecological quality standards, with turbidity, duckweed, and algal proliferation being key contributors to this problem [3]. This situation is reflective of a broader challenge in the country, as reported by the European Environment Agency, which indicates that The Netherlands has one of the poorest surface water qualities in the entire European Union. Specifically, 40% of its lakes are in a moderate ecological status, and a concerning 60% are classified as having poor or bad ecological status [21]. This not only signifies a nutrient imbalance but also severely compromises water clarity, impeding recreational use and the ecological integrity of these habitats.

To effectively tackle the issue of lake turbidity, it's crucial to target the underlying causes of turbidity as previously discussed. Over the years, a variety of strategies have been employed to mitigate this issue, each demonstrating different levels of effectiveness [16, 22]. These methods can be classified as physical, biological and chemical. Among the physical methods, dredging stands out, involving the removal of accumulated sediments from the lake bed, which not only clears the turbidity-causing particles but also restores the natural depth and ecosystem balance of the lake [23, 24]. On the biological front, biomanipulation has been a significant approach, which involves altering the composition of aquatic species, particularly fish populations, to reduce their impact on lake turbidity and promote a healthier ecosystem [25, 26]. The selection of appropriate measures should be based on a comprehensive understanding of each aquatic system. This involves conducting an in-depth assessment of the water and nutrient balance, identifying the variety of species present, with a particular emphasis on the fish populations, and carrying out a detailed cost-benefit analysis tailored to the system's usage [23].

Amongst the chemical strategies is the *"Floc & Loc"* method, which involves the addition of substances that can aggregate and precipitate suspended particles and limit nutrient availability, thereby clarifying the water. The "Floc" part of the method refers to the process of flocculation, where compounds like aluminium salts or iron chloride are added to the water. These chemicals form structures that capture and clump together fine particulate matter, including phytoplankton and other organic materials, which are major contributors to turbidity and algal blooms. This aggregation forms larger particles, known as flocs, that are more easily settled and removed through filtration. In the case that the flocs float instead of sinking, a ballast can be used to further increase their density ans sink them. The "Loc" component stands for 'locking up' of phosphorus, which is often a key nutrient fuelling algal blooms and further turbidity. Here, substances like lanthanum-modified bentonite (LMB) are used to bind phosphorus in the water column and sediments, preventing its release back into the water column and thereby limiting the nutrient availability for algal growth [15]. Besides reducing the nutrients solid compounds such as LMB or other solid P sorbents (e.g. natural soils) would also work as a ballast, settling the floated biomass [27]. This two-pronged approach effectively reduces turbidity by directly removing particulates and indirectly reducing the proliferation of algal blooms through nutrient limitation [6, 28].

The dive team De Kaaiman has been actively operating in the Nijmegen area since 1969, boasting a membership of approximately 200 members. A noteworthy feature of their diving activities is the underwater house, named the "Aquavilla", situated in the Berendonck lake, in the municipality of Wijchen - The Netherlands [29]. The Aquavilla underwater house not only serves as a diving spot but also stands as a testament to the team's commitment to advancing underwater exploration and education. This commitment to education has led the diving team to search for remedies to an increasing turbidity issue over the years as low visibility at higher depths can pose a risk to the safety of newbie divers and diminish the educational value of the divers. The particular section of the lake frequented by the Kaaiman divers is also a popular spot for fishermen. These fishermen often fish along the coast and sometimes utilise boats to enhance their fishing activities. Surrounding the lake is a golf course (see Figure 2.1), which is equipped with a drainage system. This system includes pipes that channel runoff directly into the diving area of the lake. Its contribution to water and nutrient balance of the pond is not clear.

Consequently, to further understand and address the low visibility problem in the Berendonck lake, the Kaaiman team reached out to the Science Workshop at Wageningen University and Research. The Science Shop collaborates with non-profit groups in society by organising free research projects that answer their questions, aiming to empower these groups through scientific engagement and jointly create direct, positive change. In response, the Science Shop has initiated projects to assist the Kaaiman Diving Team, and this thesis aims to contribute to those efforts.

Research Questions

In the aquatic system of the Berendonck, various interrelated factors contribute to its overall health and water clarity. From the influence of recreational activities to natural processes and anthropogenic interventions, each aspect plays a vital role in shaping the water quality and ecosystem dynamics. While many aspects can be investigated in this case study, the following thesis will concentrate specifically on the effects of diver-induced resuspension on water clarity, potential internal nutrient inputs impacting the system, and evaluate the extent to which sediment contributes to the nutrient levels in the lake. Additionally, it will explore the feasibility of using flocculants as a solution to alleviate turbidity concerns. The research questions are:

1. What impact does internal sediment phosphorus loading have on turbidity levels and its direct contribution to water clarity in the Berendonck Diving Lake?
   Hypothesis: Internal sediment phosphorus loading directly increases turbidity in the Berendonck Diving Lake by contributing to elevated chlorophyll levels and promoting algal blooms during warmer months, which absorb and scatter light within the water column.

2. What are the spatial and temporal variations in turbidity, nutrient concentrations, and visibility across different horizontal zones and depth profiles in the Berendonck Diving Lake?
   Hypothesis: During periods of stratification, turbidity and nutrient levels increase near the water-sediment interface, resulting in reduced visibility in the Berendonck Diving Lake. Horizontal visibility may vary due to diver-induced resuspension of sediments.

3. How effective is Poly Aluminium Chloride as a coagulant in reducing turbidity levels in the Berendonck Diving Lake when applied to both the water column and the underlying sediment?
   Hypothesis: PAC has the potential to reduce turbidity in the water column when applied to water while maintaining working levels of pH and can reduce resuspension when applied to the sediment, as well as increase sedimentation rates.

Methods

2.1 Field Site

Lake Berendonck is a prominent recreational site situated in the municipality of Wijchen, The Netherlands, forming part of the recreational area near Nijmegen known as Recreatiepark de Berendonck. Spanning an area of approximately 170 hectares, this vast park offers varied amenities, including a recreational lake for swimming spots, hiking trails, a golf course, and a smaller lake for diving and fishing activities. The lake itself, with a surface area of 20,000 m², depicted in Figure 2.1, was formed by sand excavation activities in the 1970s and consists of three interconnected sections. The two primary sections of interest are labelled on the map as follows: Section A, referred to as the "diving lake," is the smallest of the three, identifiable by the presence of the "Aquavilla" house, with its deepest point reaching 17 meters, refer to Appendices A.1. Section B, is termed the "reference lake," as no diving activities take place there, and shares a direct connection with the diving lake through a shallow and narrow channel. It is also connected to a sluice which regulates the water level of these three interconnected lakes, ensuring a consistent flow of groundwater from south to north. Both sections A and B are adjacent to the golf course, with Section A being encircled by it. Section A is characterised by the presence of the dive team De Kaaiman, which has been diving in the area for over 30 years [17].
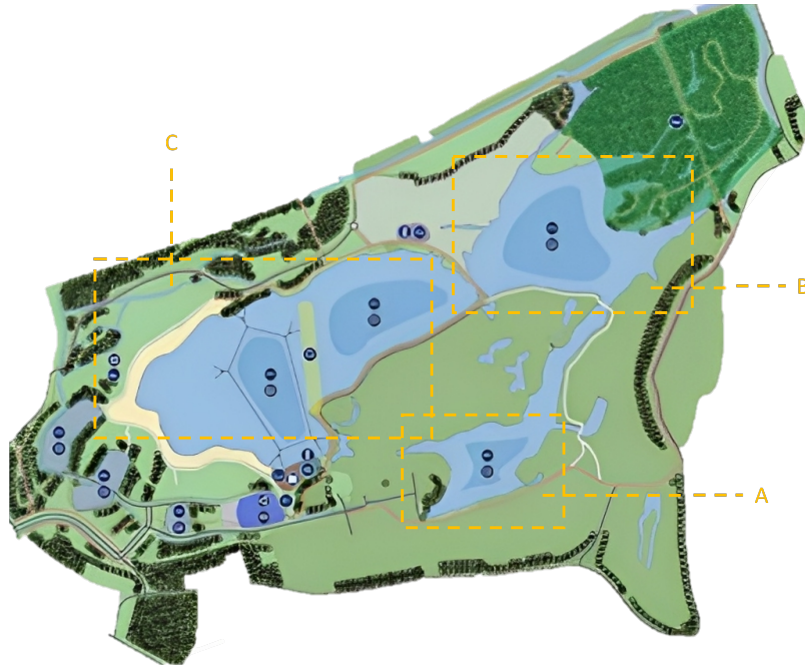
Figure 2.1: Map of Recreatiepark de Berendonck illustrating the diving lake (A), the directly connected reference lake (B) and the recreational lake (C).

2.2   Sampling and Field Measurements

Sampling and field measurements were divided between the members of the AEW chair group and the Kaaiman divers. The AEW team collected samples that required detailed laboratory evaluations and also managed the more intricate field assessments. Meanwhile, the divers were responsible for conducting direct on-site evaluations, with an emphasis on visibility measurements and on-site turbidity experiments.

2.2.1   AEW Team

Sonar measurements of the lake bed's topography were carried out with a GPS chartplotter (Lowrance HDS7) onboard a boat that navigated in a zig-zag pattern across the lake. This approach aimed to maximise coverage and enhance the resolution of the sonar data by traversing the area in narrowly spaced lines. To analyse the lake bed's topography, linear interpolation was employed using Python's SciPy library. This method was chosen for its computational efficiency and effectiveness in estimating depth values across the lake's bottom, providing a detailed bathymetric contour map based on the gathered sonar data.

To assess the extent of deep and shallow regions in the lake, the linear interpolation technique outlined previously was employed to generate precise contour lines for depths above and below the 4-meter mark. As there is no general consensus as what constitutes a shallow or deep areas of a lake, a 4-meter mark as chosen because it reflects the depth of location 2. The depth delineation was visually distinguished by employing two distinct colours to represent areas with a depth of up to 4 meters (light blue) and those exceeding 4 meters (dark blue). The image was without any background colour. The image was converted into a numpy array, and each pixel was categorised as either 'dark_blue' or 'light_blue' based on its colour intensity, using a threshold derived from the image's average grayscale value. Then, the script computed and presented the proportions of pixels falling into each category, thereby providing a quantitative assessment of the depth variation (over and under 4 meters) across the lake.

Sampling and filed measurements were conducted across three locations, each selected to represent different aspects of the lake's ecosystem: (I) the deepest point near the underwater house, to capture the primary sediment deposition zone; (II) a shallower area near the connection between the diving lake and the reference lake, to understand the influence of external water sources; and (III) a representative spot in the reference lake which has no diving activity, Figure 2.2. To assess the water quality and its spatial and temporal variability, we carried out water sampling at these designated locations during the months of November and December of 2023, and January of 2024. In location 1, water samples were collected at vertical intervals of 2 meters, from the surface down to the sediment interface, using UWITEC water samplers. Surface water was collected at Location 2 and Location 3. Additionally, Secchi disk measurements, electrical conductivity (EC) (Hach E1103), and dissolved oxygen (DO) (Hach DO013) were measured at each location. During the fieldwork done on the 12.12.2023, surface water was collected from a fourth location - an inflow drainage pipe that was operational during the fieldwork.

To investigate internal nutrient loading, six sediment cores were collected from locations 1 and 2, and four sediment cores from location 3. Due to sampling error, 2 cores were lost at location 3. Sampling was done with the use of sediment cores (60 cm height, 6 cm diameter) using a UWITEC gravity corer once the lake's water was confirmed to be in a mixed state, ensuring the bottom layer was not anoxic. This timing ensured that the sediment samples represented typical oxygenated lake conditions. This approach facilitates clearer comparisons with induced anoxic conditions in the laboratory, aiding the understanding of oxygen's impact on sediment nutrient dynamics. Concurrently, one additional sediment core was sampled from each of the three locations and sliced into three sections; 0 - 5 cm, 5 - 10 cm, 10 - 15 cm.

2.2.2   Diving Team

To assess the impact of re-suspension in the lake, divers from the club De Kaaiman conducted underwater observations. A protocol was established wherein divers measured both the vertical and horizontal visibility of the water at various depths and locations using a Secchi disk. Alongside these visibility measurements, the divers collected water samples for analysis of turbidity using a turbidity meter at the diving site. Secchi disk measurements were taken before any diving activity to establish a baseline and after divers
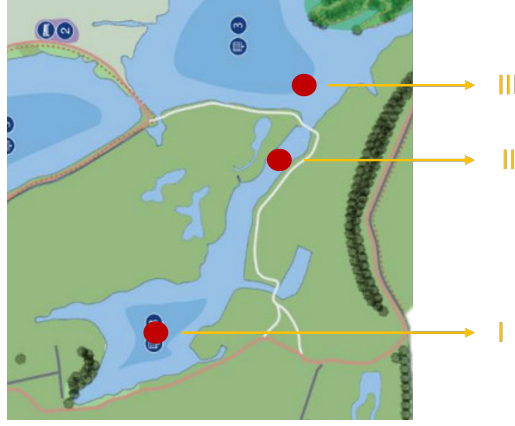
Figure 2.2: Map of Recreatiepark de Berendonck illustrating the locations chosen for sampling. Location I: the deepest part of the lake, location II: a shallower part with connection to the reference lake, location III: Reference Lake.

conducted their activities to evaluate the degree of sediment disturbance. By comparing the visibility measurements pre- and post-diving, it was possible to determine the impact of diver-induced re-suspension on water clarity. Moreover, the goal was to identify if there are areas of the lake's sediment that have higher re-suspension rates. The divers utilised standardised equipment and protocols, Appendices A.1, ensuring consistency across all measurements.

2.3 Laboratory Analysis

2.3.1 Water

Laboratory analyses of the water samples focused on key water quality indicators including turbidity, suspended solids, chlorophyll-a concentrations, and both filterable and total nutrients. After collection, the samples were analysed on the same or the following day and were kept in the fridge at 4 °C until analysis. The determination of pH was done by a glass electrode (WTW Sentix 41). Electrical conductivity, indicative of the water's ionic activity and salinity, was measured using a conductometric electrode (WTW Tetracon 325), chlorophyll-a was determined through spectrophotometry (WALZ PHYTO-PAM), and turbidity was measured by a turbidity meter (Hach 2100P). Filtered (GF/F, 0.45 μm) and unfiltered 50 mL subsamples were stored in the freezer at -17°C until nutrient analysis (total nitrogen (TN), ammonia (NH_3), nitrite (NO_2^-)/nitrate (NO_2^-), ortho phosphate (PO_4) and total phospate (TP)) with a segmented flow autoanalyser (SFA) (Skalar - SAN++).

Suspended solids (dry and ash weight) were measured by filtering the water samples through a GF/F filter (0.45 μm), weighing them after drying at a controlled temperature of 105°C overnight to obtain the dry weight (M_{dry}), and incinerating at 520°C for 3 hours to measure the ash weight (M_{ash}), refer to formulas 2.1 and 2.2. The filters were weighted , dried and incinerated on a aluminium dish. The weight of the filters and aluminium dish was initially determined after drying them at 550°C for 3 hours to obtain their initial weight (M_0). The volume of filtered water depended on the volume that it took to saturate the filter and it varied by sample, this volume was measured with a measuring cylinder (V).

$$DW(g/L) = \frac{M_{dry} - M_0}{V} \tag{2.1}$$

$$AW(g/L) = \frac{M_{ash} - M_0}{V} \tag{2.2}$$

2.3.2 Sediment Cores

Following collection, the sediment core samples were incubated in a controlled laboratory setting; at 4 - 7 °C and darkness. They were stored in a temperature-regulated environment set to reflect the lake's average bottom temperature during the warmer months, which is the typical period for anoxia. To mimic the low-light conditions of the hypolimnion during stratification, which often leads to anoxic conditions, the cores were kept in complete darkness. Three cores from each location were purged with nitrogen gas until through a stone diffuser O_2 concentration was lower than 0.5 mg/L to create an anoxic atmosphere, displacing oxygen to cease aerobic processes. This anoxic environment was critical to studying the dynamics of phosphorus release and its chemical speciation in conditions conducive to eutrophication [30]. If oxygen levels in the anoxic cores exceeded 0.5 mg O_2/L, nitrogen was bubbled to lower the concentration to 0.5 mg O_2/L or less. Conversely, another set of three cores from each location was maintained under oxic conditions.

Once a week, over a period of four weeks, 40 mL samples of supernatant were collected from each core for analysis. 20 mL of these samples were filtered through a 0.45 µm unit filter for ortho-phosphate (P-PO$_4$) measurements. Additionally, parameters such as turbidity, pH, oxygen (concentration and saturation), and electrical conductivity (EC) were monitored in the water column of each core. The analysis of the supernatant was consistent with the methodology applied to the water sample analysis described earlier in section 2.3.1. After each sampling event, 40 mL of distilled water was added to the cores to replace the volume removed. The collected samples were then stored at -17°C in a freezer until nutrient analysis could be conducted with the SFA (Skalar - SAN++).

To quantify ortho-phosphate (P-PO$_4$) concentrations in water samples from the sediment cores, a molybdate assay through spectrophotometric method was employed, utilizing a calibration curve established with eight phosphate standards of known concentrations. For the preparation of the phosphate reagent solution, a mixture of Solution A (Ammonium Molybdate and sulfuric acid) and Solution B (Antimony Potassium Tartrate) was combined with Ascorbic acid. Samples were processed by adding 0.5 ml of the phosphate reagent solution to 4.5 ml of each water sample, followed by thorough mixing. The absorbance was then measured at 690 nm after a 12-minute incubation but within 40 minutes to ensure accuracy. The calibration curve, plotted with phosphorus concentration against absorbance, was generated in Excel, and a linear regression equation derived from this curve was used to calculate the unknown phosphorus concentrations in the water samples.

To calculate the flux per day (d) per area in meters (a), the difference between mean P-PO$_4$ (ug/core) of the cores of the last day of the experiment (P2) was subtracted from the mean value of the first day of the experiment (P1) and divided by the area of the core and the number of days the experiment ran, Equation **??**.

$$\frac{P2 - P1}{a \cdot d} \tag{2.3}$$

For Location 1, to calculate the annual P-PO$_4$ release, we assumed that the deep part of the lake is under oxic conditions for 90 days of the year and under anoxic conditions for 275 days of the year. We also took into account the analysis of the bathymetric contour map of the lake to determine shallow (under 4 meters depth) and deep parts (over 4 meters depth) of the lake, represented in Equations 2.4.

$$S = D_{\text{mix}} \times R_{\text{oxic}} + D_{\text{strat}} \times (A_{\text{deep}} \times R_{\text{anoxic}} + A_{\text{shallow}} \times R_{\text{oxic}}) \tag{2.4}$$

S : Total annual sediment release per square meter (µg)

D_{mix} : Number of days the lake is in a mixed state

D_{strat} : Number of days the lake is in a stratified state

A_{deep} : Proportion of the lake that is deep

A_{shallow} : Proportion of the lake that is shallow

R_{oxic} : Sediment release rate under oxic conditions (µg/m²/day)

R_{anoxic} : Sediment release rate under anoxic conditions (µg/m²/day)

2.3.3 Sediment Fractions

To understand the sediment composition and its potential environmental impact, dry weight measurements were conducted to establish a baseline for the other analyses, allowing for comparisons and calculations on a uniform basis. The determination of density provided insights into the sediment compaction and its potential for water and nutrient retention. Loss on drying (LOD) at 105 °C and Loss on Ignition (LOI) at 550 °C was employed to quantify the amount of water and volatile organic matter, which plays a role in the sediment's chemical reactions and its influence on water quality. Furthermore, a sequential phosphorus extraction (according to Psenner procedure was done on a sample from each location at each sediment fraction to determine the total phosphorus load in the sediment that may potentially be released into the water as conditions change.

LOI and LOD

Known quantities (aprox. 5g) of the sediment were dried in crucibles at 105 °C for 48 hours, and the mass loss was calculated as per Equation 2.5, where M_0 is the initial mass in grams of the initially weighed crucibles, and M_{dry} is the mass after drying. The dried samples were then ignited at 550 °C for 3 hours, and the mass loss was determined following Equation 2.6, with M_{ash} being the mass after ashing.

$$LOD(\%) = \frac{M_0 - M_{dry}}{M_0} \cdot 100\% \tag{2.5}$$

$$LOI(\%) = \frac{M_{dry} - M_{ash}}{M_{dry}} \cdot 100\% \tag{2.6}$$

Density

To accurately measure sediment density, the soil was first thoroughly mixed to ensure consistency throughout the experiment. A 10 mL syringe, modified by cutting off the narrower end, was used to precisely determine both the volume and mass of the sediment. The final volume of the syringe after being cut was 9.5 mL. Careful attention was given to filling the syringe to the 9.5 mL mark with sediment, ensuring no air pockets remained that could skew the results. Once filled, the syringe packed with sediment was weighed on a digital scale. The mass of the sediment was calculated by subtracting the weight of the empty syringe, previously recorded, from the weight of the syringe now containing sediment. The density was calculated by using the formula:

$$density = mass(g)/9.5mL \tag{2.7}$$

Sequential Extraction

To investigate soil phosphorus (P) fractions and sorption dynamics, a sequential extraction following AEW protocol based on the Psenner extraction method [31] was conducted, refer to Appendices A.3 for the full

procedure. A sub-sample (4g) from each core fraction was treated with solutions of increasing strength, sequentially releasing P for analysis at each step, detailed in table 2.1. The procedure began with extracting loosely adsorbed P, followed by redox-sensitive P from Fe-hydroxides and Mn-compounds, and then P bound to metal oxides. Further steps released inorganic P from carbonates and organic P, with the final acid digestion yielding total P, including refractory forms.

Table 2.1: Phosphorus Partitioning via Sequential Extraction: Detailing the methodologies used in sequential phosphorus extraction and their associations with the material's distinct phosphorus reserves. SRP: soluble reactive phosphorus and TP: total phosphorus.

Phase	Solution	P-analysis	Corresponding sorbent substrate
1	O_2-free distilled water	SRP	Fe & $CaCO_3$ surfaces; loose
2	O_2-free 0.11 M $Na_2S_2O_4$/$NaHCO_3$	SRP & TP	Fe-hydroxides & Mn-compounds
3	0.1 M NaOH	SRP & TP	Clay-minerals & metal(Al)-oxides, organic P
4	0.5 M HCl	SRP & TP	Carbonates & P-containing minerals
5	2 M H_2SO_4	SRP	Refractory P

Equation 2.8 was used to calculate the amount of P (TP and P-PO_4) in the sediment fractions in mg P/g sediment). The results from 2.3.3 were used to determined the dry weight (DW) of the sediment.

$$P_{\text{sed}} = \frac{[P_f] \times V_{\text{extract}}}{DW} \tag{2.8}$$

In which $P_{\text{sed}} = [P]$ in sediment ($mgPg^{-1}DW$), $P_f = [P]$ in fraction ($mgPmL^{-1}$), $V_{\text{extract}} =$ volume extractant (mL), $DW =$ dry-weight sediment (g).

The potentially releasable phosphorus (P) from the top 10 cm of the sediment comprised the sum of the first three phases of the sequential extraction: pore water P, Fe/Mn-bound P, reductively soluble organic P, and organic P.

2.4 Coagulant Experiment

2.4.1 Water

Water samples, encompassing the observed range of turbidity in the lake, were treated with Poly Aluminium Chloride (CALDIC - CALFLOCK P-14. $1.33g/cm^3$, 7.2% Al). The selection of turbidity levels for the study was based on the lowest and highest readings recorded during the sampling period. The lowest turbidity, measured in the surface water, was approximately 2.6 Nephelometric Turbidity Units (NTUs). To replicate higher turbidity conditions, plankton was concentrated using a seston net with a 45 µm mesh, resulting in a turbidity of 23.4 NTU. This water was then passed through a 125 µm sieve to eliminate larger particles that quickly settle, ensuring the remaining turbidity more accurately reflected the general conditions of the water column, which adjusted the turbidity to 13 NTUs. An intermediate turbidity level, approximately 6 NTUs, was established by mixing samples with turbidities of 2.6 and 13 NTUs. Consequently, the turbidity levels tested were 2.59, 6.30, and 13.30 NTUs. To evaluate the efficacy of PAC at these turbidity levels, five concentrations of PAC (0, 1, 2, 4, 8, and 16 mg Al/L) were added in 100 ml of water sampled using 100 mL glass tubes. Following PAC treatment, the samples were allowed to settle for 1 hour, after which 10 mL samples from the top and from bottom of the tubes were collected and analyzed for turbidity. Measurements of electrical conductivity (EC) and pH were also performed before and after the flocculation process, directly within the tubes and followed the same procedure as the water analysis in section 2.3.1.

2.4.2 Sediment

To assess the efficacy of PAC directly applied to the sediment, four sediment cores from location 1 were reserved for this experiment. Two cores were designated to investigate the impact of PAC in the sediment, and two were employed as controls. A specific concentration of PAC was selected, based on the average internal phosphorus (P-PO_4) loading of location 1, deduced from the sediment core experiment described in 2.3.2. PAC was added in a molar Al:P ratio of 10:1 ([32]) resulting in 30.56 mg of PAC were added per core. The introduction of PAC to two cores was performed utilizing a syringe needle connected to a syringe through a tube. This tube was stabilised with a metal rod to aid in the needle's penetration into the sediment. PAC was evenly administered within the first 10 cm of the sediment. Following application, PAC was allowed to react for 30 minutes. The sediment was subsequently resuspended for one minute by the bubbling of O_2 on the first centimetres of the sediment's surface. The same flow of O_2 was used for all cores. Turbidity levels were measured prior to the experiment's initiation, during the resuspension of the sediment, and at 15 and 30 minutes post-resuspension. pH levels were measured at the end of the experiment. The methods for turbidity and pH measurements followed that of section 2.3.1.

2.5 Data Analysis

Microsoft Excel was used to clean, analyse, and prepare the data. Python 3 and Latex were used to visualise the data through graphs and tables and to perform all statistical analysis. Statistical analysis consisted of simple descriptive and inferential statistics.

Results

3.1 Lake Profile

The bathymetric survey of the lake, as represented by Figure 3.1, shows a depth gradient with a maximum measured depth of 16.8 meters. The spatial distribution of depth indicates a central basin, with the deepest point located towards the northern quadrant. Shallower regions predominantly skirt the southern and eastern perimeters of the lake, where depth readings rapidly ascend from deep blue to red on the colour scale. Contour lines are denser around the deep central area, suggesting a steep-sided depression, while more widely spaced lines towards the edges imply a gentler incline of the lakebed. No significant anomalies were observed in the peripheral shallows, indicating a consistent slope from the banks towards the central highest depth point.
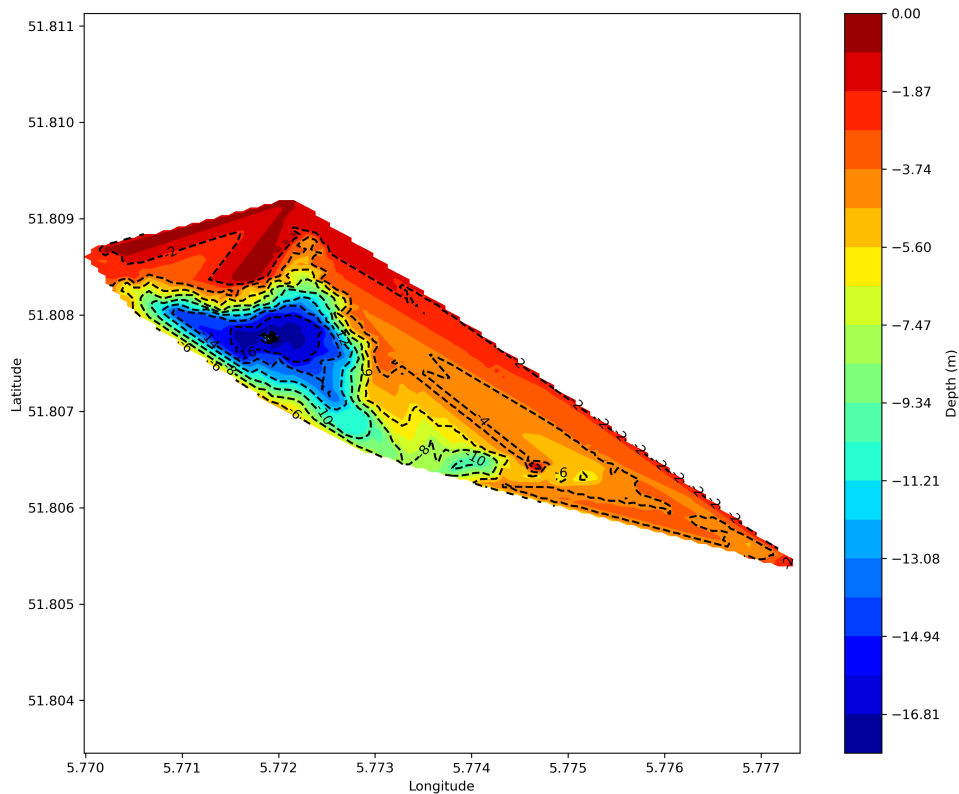
Figure 3.1: Bathymetric contour map of the diving lake illustrating depth variations, with the deepest point centrally located, highlighted by a steep gradient from red (shallow) to blue (deep). Contour lines indicate the topography of the lakebed, with the colour scale representing depth in meters.

The adjusted depth profile of the diving lake followed by pixel analysis estimated that 67.25% of the lake's surface area is comprised of deeper waters, indicated by dark blue colouring, while the remaining

32.75% constitutes the shallower regions, marked in light blue. This quantitative assessment is based on a depth threshold of 4 meters, as shown in the contour mapping in Figure 3.2.
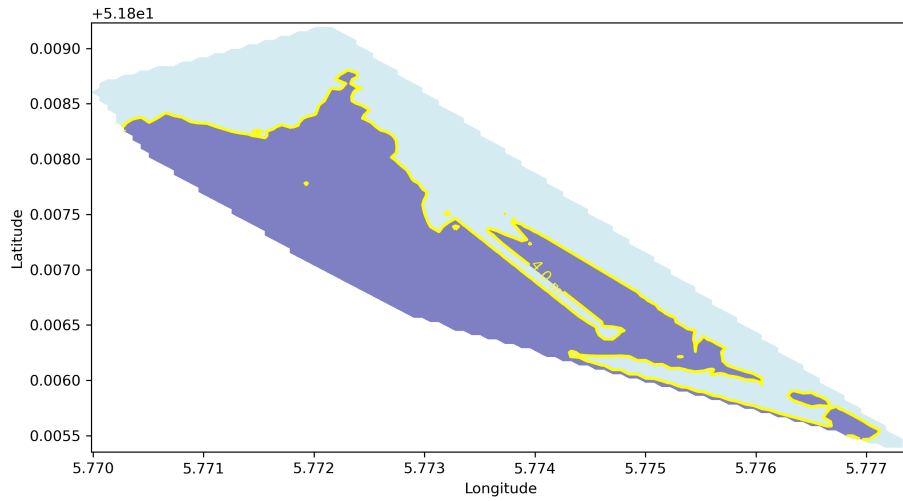
Figure 3.2: Adjusted Depth Profile of diving lake, highlighted in light blue colour are the areas with depths up to 4 meters (shallow zones) versus those deeper than 4 meters, in dark blue colour. Dark blue pixels: 67.25%, Light blue pixels: 32.75%.

3.2   Water

The analysis of water samples taken from Berendonck Lake on November 23, 2023, as presented in appendices Table A.1, revealed that a decrease in dissolved oxygen levels and temperature with increased depth, with hypoxic conditions observed below 11 meters at Location 1. Concurrently, turbidity levels notably intensified beyond 11 meters, aligning with an increase in chlorophyll-a concentrations at the greatest depths sampled, Figure 3.3. The pH across the samples remained relatively consistent, ranging from 6.6 at the surface to 7.15 at a depth of 16 meters. Electrical conductivity showed variations from 382 to 428 µS/cm, suggesting changes in ionic composition with depth.

The evaluation of aquatic samples obtained on December 12, 2023, demonstrated a more homogeneous water column at Location 1, in contrast to the heterogeneity observed in the preceding assessment, appendices Table A.2. Values for O_2, temperature, chl-a pH and EC presented minimal variations with increasing depth. Turbidity, TSS and VSS were generally low, except for a notable spike at the 16-meter depth, where values rose sharply. Oxygen levels gently declined from 5.03 mg/L at the surface to 3 mg/L at 14 meters.

The parameter measurements taken from samples collected on January 25, 2024, at Location 1 showed minor variations with depth, appendices Table A.3. From the surface down to a depth of 16 meters, there was a slight decrease in both temperature and oxygen levels. Specifically, the temperature dropped from 5 °C to 4.6 °C, and the oxygen concentration decreased from 8.15 mg/L to 7.46 mg/L. pH, EC, TSS, VSS and chl-a showed no significant variations across depth. Turbidity values peaked at a depth of 6 meters at 5.59 NTU.

Figure 3.3 displays the variation in temperature and O_2 levels at different depths recorded during the three distinct sampling events. In the first sampling event (continuous line), there is a pronounced reduction in both temperature and O_2 concentrations between the depths of 10m and 12m. For the second event (dashed line), the temperature remains relatively stable across depths, with a sudden decline around 11 meters, whereas O_2 levels decrease steadily after 6 meters. The third event (dash-dot line) shows a gradual decrease in temperature with increasing depth and a consistent drop in O_2 concentrations throughout the water column.
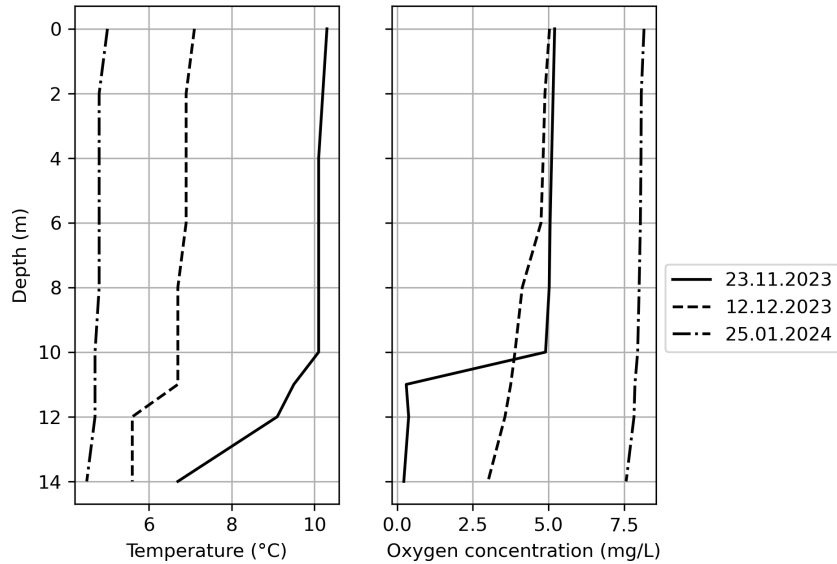
Figure 3.3: Temperature (°C) and oxygen concentration (mg/L) profiles at various depths at Location 1 of the diving lake, recorded on the three different sampling dates.

Figure 3.4 illustrates the profiles of turbidity and chlorophyll-a (chl-a) at different depths during the three sampling events. During the first sampling event (continuous line), there was a significant peak in turbidity at around 14 meters depth, with a corresponding peak in chl-a concentration at approximately the same depth. The second event (dashed line) displayed a slight peak in turbidity at 6m before gradually decreasing until 14 meters, while chl-a showed a modest increase in values until 11 meters followed by a sharp decrease from 11 to 14 meters. The third event (dash-dot line) demonstrated similar trends for both turbidity and chl-a: a gradual decrease in concentrations with increasing depth.
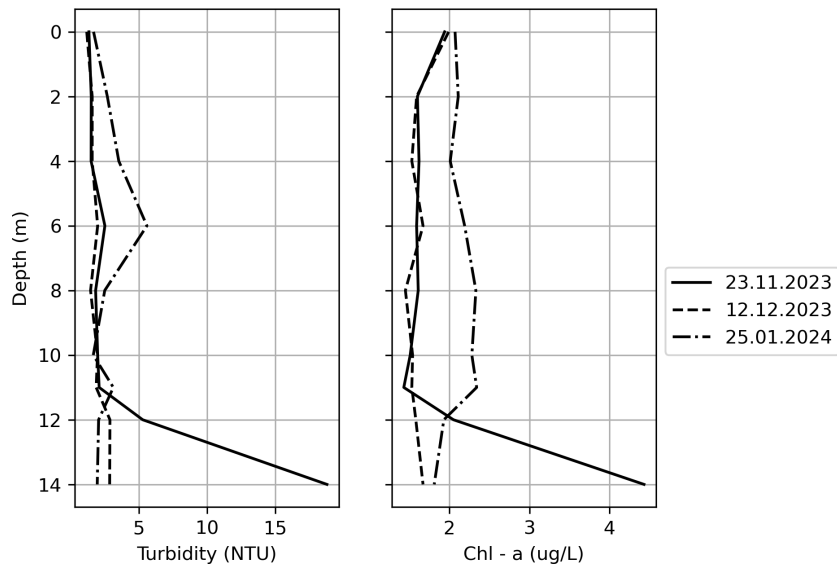
Figure 3.4: Vertical profiles of turbidity (NTU) and chlorophyll-a (μg/L) concentration at Location 1 of the diving lake, captured on the three different sampling dates.

Total phosphorus (TP) and phosphate (P-PO$_4$) levels remained relatively unchanged throughout the water column for all three sampling events, with $P-PO_4$ generally below 50 μg/L and TP generally below 0.1 mg/L, refer to Table A.4, Table A.5 and Table A.6 in the appendices. However, an exception occurs in the samples from November 23, 2023, where both phosphorus species show a rapid increase after

12-meter depth, as illustrated in Figure 3.5. $P-PO_4$ levels increase from 24.8 μg/L at 11 meters to 470.52 μg/L at 14 meters and 422.76 μg/L at 16 meters. Similarly, TP levels increase from 0.03 mg/L at 11 meters to 0.48 mg/L at 16 meters. These results coincide with the presence of a thermocline and oxicline after the 11-meter depth, as shown in Figure 3.3.
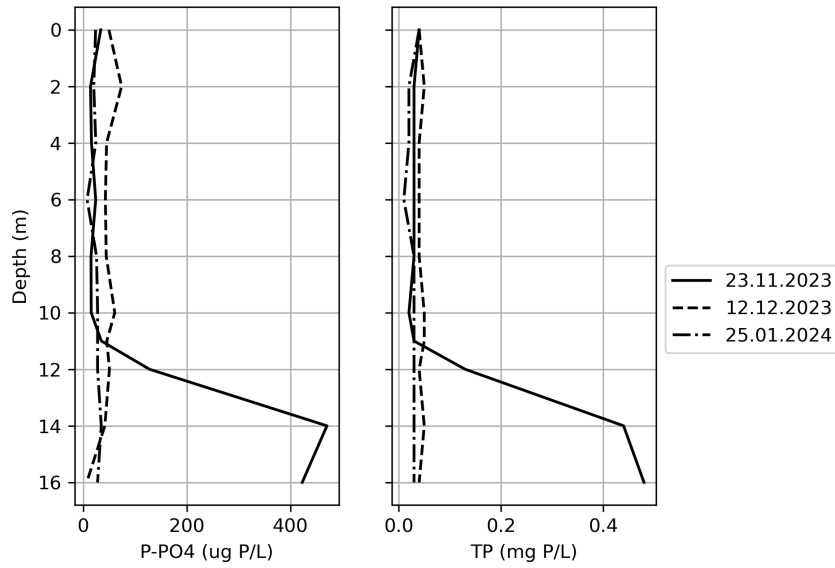
Figure 3.5: Vertical profiles of P-PO$_4$ (μg P/L) and TP (mg P/L) concentration at Location 1 of the diving lake, captured on the three different sampling dates.

Total nitrogen (TN), ammonia (NH$_3$), and nitrite-nitrate (NO$_2^-$ − NO$_3^-$) concentrations are profiled from the surface down to a depth of 16 meters, based on three sampling events, Figure 3.6. The concentration of TN shows an increasing trend from the surface downwards, with the highest levels generally occurring at greater depths. Notably, on November 23 and December 12, 2023, TN levels rise sharply after 11 and 14 meters depth respectively. Ammonia concentrations are consistently below 1 mg N/L from the surface down to 11 meters, after which there is a similar trend to TN rise. With the exception of the samples from January 25, 2024, nitrite-nitrate levels remain generally below 0.4 mg N/L at all depths, there was a notable sharp decrease in concentration for samples from December 12, 2023 after the 12-meter mark.
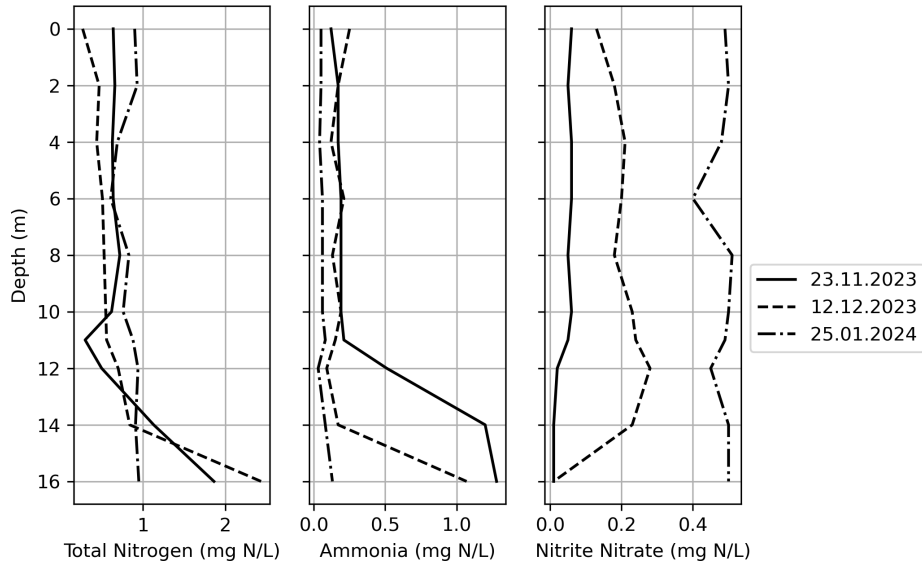
Figure 3.6: Vertical profiles of TN (mg N/L), Ammonia (mg N/L) and Nitrite Nitrate (mg N/L) concentration at Location 1 of the diving lake, captured on the three different sampling dates.

An ANOVA analysis was conducted across the various water quality parameters (including dissolved oxygen, pH, and turbidity) across the three locations (Figure A.7) and it showed no statistically significant differences, with all p-values well above the conventional threshold of 0.05. However, the reliability of these results may be compromised by the small sample size of only three observations per location, which limits the statistical power of the tests and the precision of the variance estimates. The results from the sample collected at the inflow drainage pipe did not show major differences from the other three locations. However, even if presenting small differences, values of Total P and P-PO$_4$ were about 50% higher when comparing surface water from Location 1 and the water from the drainage pipe, refer to Table A.5.

Unfortunately, due to the cold weather and the time required to integrate new diving practices, such as sample collection and Secchi disk measurements, the Kaaiman divers were not able to collect extensive data. Diving events took place on three dates: March 3, 2024; March 9, 2024; and April 1, 2024 and were concentrated on locations around the underwater house at Location 1. During the last dive, we learned more about the adaptations the diver are making to be able to carry out the field measurements in a more efficient way. As of that date, they had made a support for the collection bottles and another support for the secchi disk to be attached to their suits, leaving their hands free. None of the measurements were taken before and after diving activities on the same diving event, so the comparison of those results cannot be done. Some of the measurements are also incomplete. The available data is presented in Table 3.1. The recorded horizontal visibility ranged from 1.35 to 3.25 meters, vertical visibility from 2.4 to 3.2 meters, and turbidity readings from 1.57 NTU to 6.73 NTU. Up to a depth of 4 meters, the average horizontal visibility was 1.51 meters, the average vertical visibility was 2.60 meters, and the average turbidity was 2.68 NTU. At depths greater than 4 meters, the average horizontal visibility was 2.48 meters, the average vertical visibility was 2.87 meters, and the average turbidity was 4.00 NTU.

Table 3.1: Visibility (m) (horizontal and vertical) and turbidity (NTU) measurements taken by the members of the Kaaiman diving team during the months of March (M) and April (A) of 2024.

Depth (m)	Month	Horizontal Vis. (m)	Vertical Vis. (m)	Turbidity (NTU)
1	M	-	-	1.84
1	M	-	-	4.8
3	A	1.66	2.6	1.57
4	M	1.35	2.6	2.51
6	M	3.3	2.4	-
6	A	1.7	2.7	3.47
6	A	1.66	2.6	5.76
7.6	M	2.15	3.25	1.71
8	A	-	-	5.75
9	M	2.35	3.2	2.29
9	A	-	-	2.2
9.5	M	2.9	2.8	4.1
10	A	-	-	6.73

3.3 Sediment

Orthophosphate $(P-\mathrm{PO_4})$ concentration in cores taken from Location 1 increased each week during the four weeks of the sediment core experiment. Cores maintained under anoxic conditions exhibited a higher overall increase in $P-\mathrm{PO_4}$ concentration compared to cores kept in oxic conditions, as shown in Figure 3.7. Values from anoxic cores reached $P-\mathrm{PO_4}$ averaged concentration levels of 363.65 μg/L (SD = 130.36) at the end of week 4, compared to 172.65 μg/L (SD = 23.66) for oxic cores during the same period. This pattern was not observed at Location 2, Figure 3.8, where the concentration of P-PO$_4$ also increased from week one onwards but exhibited a much lower range of values at the end of week 4, 14.20 μg/L (SD = 12.12) for anoxic cores and 16.32 μg/L (SD = 5.61) for oxic cores. Results from Location 3 showed that (P-PO$_4$) concentrations rose to 151.08 μg/L (SD = 199.57) in the anoxic cores while levels of (P-PO$_4$) in the oxic cores remained almost unaltered 19.38 μg/L (SD = 14.52), Figure 3.9.
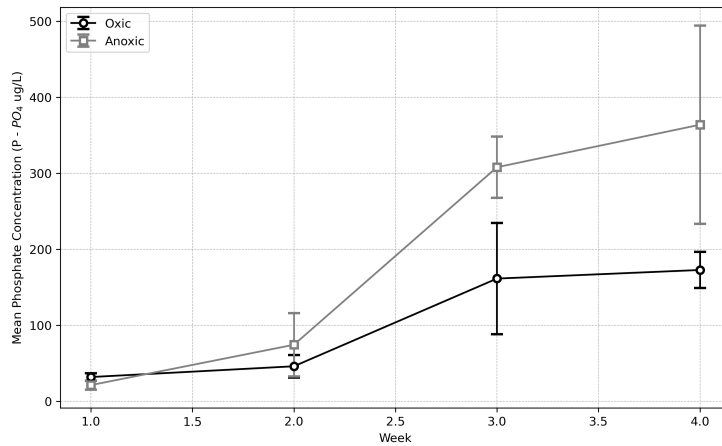
Figure 3.7: Averaged phosphate concentration (P-PO$_4$ μg/L) in the water column of three anoxic and three oxic cores from Location 1 over a time of four weeks. The error bars indicate variability within the dataset.
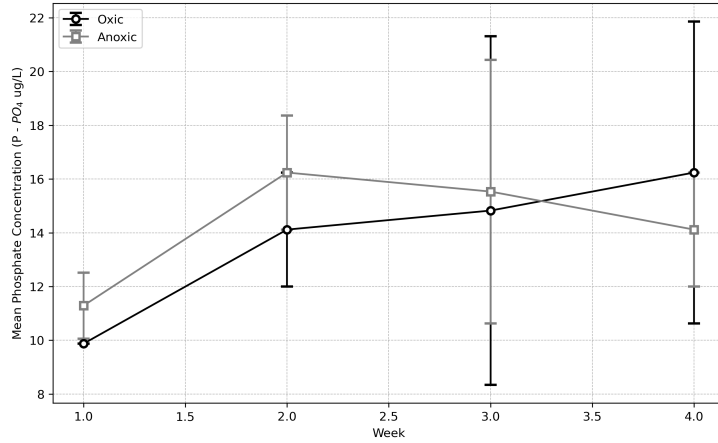
Figure 3.8: Averaged phosphate concentration (P-PO$_4$ μg/L) in the water column of three anoxic and three oxic cores from Location 2 over a time of four weeks. The error bars indicate variability within the dataset.
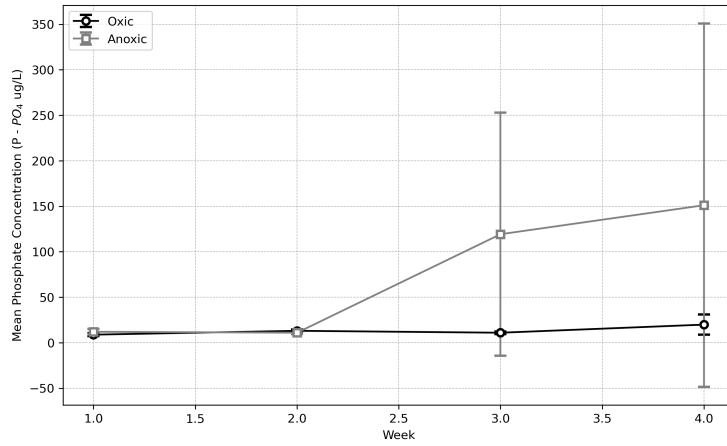
Figure 3.9: Averaged phosphate concentration (P-PO$_4$ μg/L) in the water column of two anoxic and two oxic cores from Location 3 over a time of four weeks. The error bars indicate variability within the dataset.

In Figure 3.10, the observed fluxes indicate distinctive patterns across the sampled locations. For Location 1, anoxic conditions yielded a markedly high phosphate flux, surpassing 4000 $ug \cdot m^{-2} \cdot d^{-1}$, which starkly contrasts with the lower flux recorded under oxic conditions. Location 2 showed little variation between oxic and anoxic conditions with values under 80 $ug \cdot m^{-2} \cdot d^{-1}$. Meanwhile, Location 3 showed high values for anoxic conditions around 2000 $ug \cdot m^{-2} \cdot d^{-1}$. The annual P-PO$_4$ release based on values from the sediment core analysis from Location 1 and Location 2, using Equation 2.4, was calculated to be 0.759 $g \cdot m^{-2}$ per year.
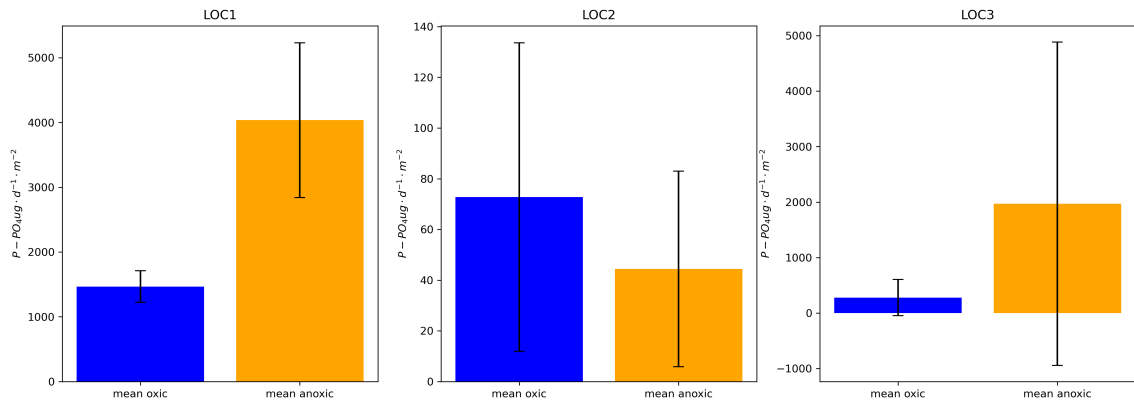
Figure 3.10: Comparative analysis of mean daily phosphate flux ($P-\mathrm{PO_4}$ in $mg \cdot m^{-2} \cdot d^{-1}$) across three locations (LOC1, LOC2, LOC3), contrasting oxic and anoxic environmental conditions, with error bars representing the standard deviation of the mean.

An analysis of Figure 3.11, Figure 3.12, and Figure 3.13 reveals a consistent trend in the variation of organic matter content with sediment depth at the three different locations. The data revealed an inverse relationship between both Loss on Ignition (LOI) and Loss on Drying (LOD) with density. As presented in Table A.8, a decrease in LOI percentages with increasing depth was evident across all three locations: from 90.27% to 64.10% in Location 1, 82.88% to 76.64% in Location 2, and from 74.06% to 52.32% in Location 3. Concurrently, soil density increased with depth, from 1.06 to 1.21 g/mL in Location 1, 1.09 to 1.22 g/mL in Location 2, and 1.13 to 1.21 g/mL in Location 3, concurrent with a decrease in LOD associated with greater soil compaction.
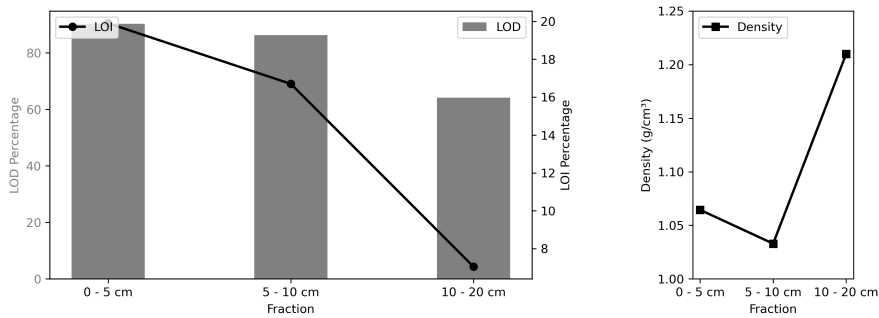
Figure 3.11: Left - Dual-axis bar graph showing Loss on Drying (LOD) and Loss on Ignition (LOI) as percentages. Right - line graph showing sediment density, for three sediment depth fractions at Location 1.
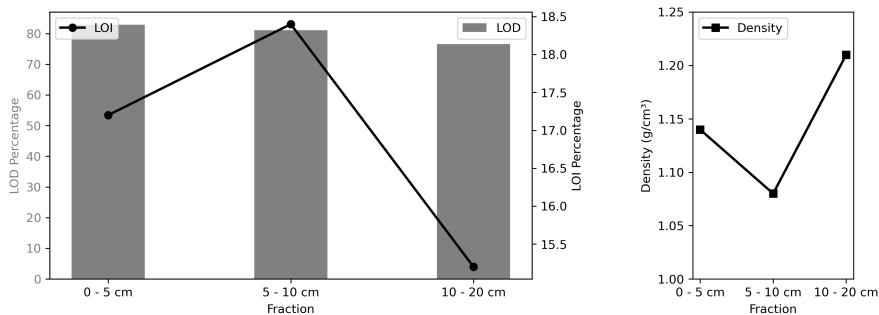
Figure 3.12: Left - Dual-axis bar graph showing Loss on Drying (LOD) and Loss on Ignition (LOI) as percentages. Right - line graph showing sediment density, for three sediment depth fractions at Location 2.
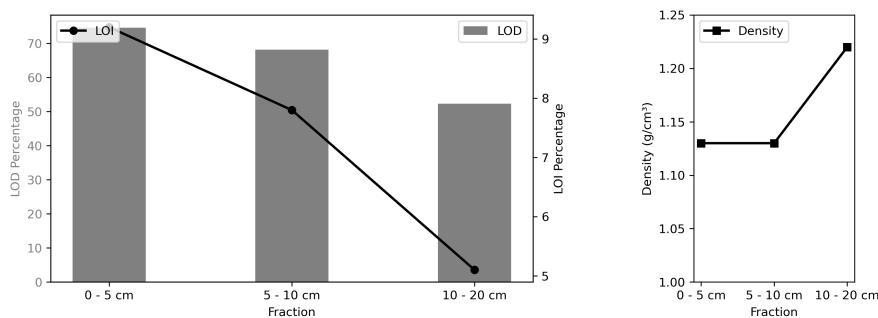
Figure 3.13: Left - Dual-axis bar graph showing Loss on Drying (LOD) and Loss on Ignition (LOI) as percentages. Right - line graph showing sediment density, for three sediment depth fractions at Location 3.

The potential releasable phosphorus (PRP) from the top 10 cm of sediment from Location 1 (1.853 mg P/g DW sediment) is over three times higher than that from Location 2 (0.592 mg P/g DW sediment) and almost six times higher than from Location 3 (0.250 mg P/g DW sediment). The difference between Location 2 in the diving lake and Location 3 in the reference lake becomes more significant when considering that the depth of the collected sediment was about 5 meters at Location 2 and about 10 meters at Location 3.

Figures 3.14 to Figure 3.16 display the concentrations of six identified forms of phosphorus, each allocated to a specific phase, across different depths of sediment. These figures can be used to understand the potential availability of phosphorus for biological processes in the sediment, as some forms are more readily available than others. Table A.9 in the appendices distinguish the values of these six phases into the PRP phase and refractory phase.

The highest phosphorus concentrations are consistently found in the top 0-5 cm layer of sediment at all three locations, with a notable decrease in concentration as depth increases, indicating that phosphorus is most readily available near the sediment-water interface. At Location 1, PRP is the predominant form from 0 to 10 cm depth, suggesting that Al and Ca metals may play a crucial role in phosphorus binding in the sediment, thereby influencing its bio-availability and potential for release. Location 1 has the highest concentrations of both potentially releasable phosphorus (PRP) and refractory phosphorus, indicating a greater potential for phosphorus mobility. In contrast, Locations 2 and 3 exhibit lower PRP concentrations, implying a reduced risk of phosphorus mobilisation from the sediments. Furthermore, Locations 2 and 3 have a larger proportion of Refractory P compared to PRP, indicating that the phosphorus present is predominantly in a more stable and less bio-available form.
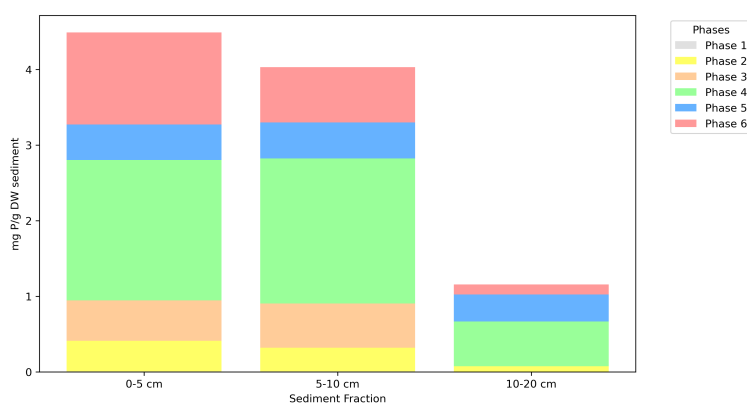
Figure 3.14: Distribution of phosphorus phases across sediment depths (0-5 cm, 5-10 cm, 10-20 cm) from Locations 1. Phase 1 = Pore water, Phase 2 = Fe, Mn bound P, Phase 3 = NRP (Non-reactive phosphorous) NaOH, Organic P, Phase 4 = SRP (Soluble reactive phosphorous) NaOH Al/Ca bound P, Phase 5 = Carbonates and P-Containing Minerals, Phase 6 = Refractory P.
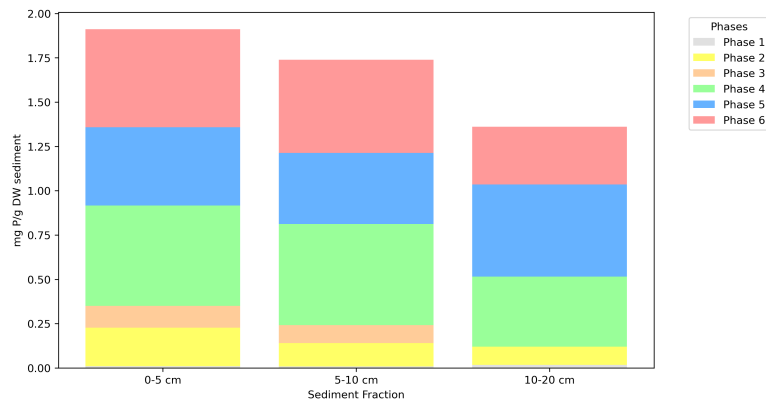
Figure 3.15: Distribution of phosphorus phases across sediment depths (0-5 cm, 5-10 cm, 10-20 cm) from Locations 2. Phase 1 = Pore water, Phase 2 = Fe, Mn bound P, Phase 3 = NRP (Non-reactive phosphorous) NaOH, Organic P, Phase 4 = SRP (Soluble reactive phosphorous) NaOH Al/Ca bound P, Phase 5 = Carbonates and P-Containing Minerals, Phase 6 = Refractory P.
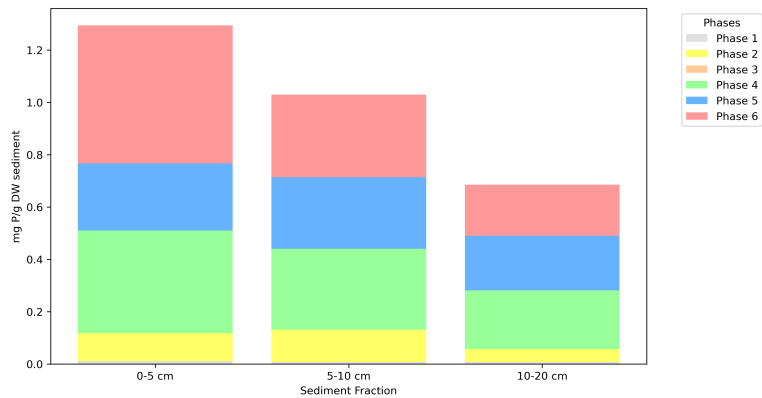
Figure 3.16: Distribution of phosphorus phases across sediment depths (0-5 cm, 5-10 cm, 10-20 cm) from Locations 3. Phase 1 = Pore water, Phase 2 = Fe, Mn bound P, Phase 3 = NRP (Non-reactive phosphorous) NaOH, Organic P, Phase 4 = SRP (Soluble reactive phosphorous) NaOH Al/Ca bound P, Phase 5 = Carbonates and P-Containing Minerals, Phase 6 = Refractory P.

3.4 Coagulant Experiment

3.4.1 Water

The application of PAC to water is presented in Figures 3.17, 3.18, and 3.19 for initial turbidity concentrations of 2.59 NTU, 6.3 NTU, and 13.3 NTU, respectively. The dark grey bars represent the levels of turbidity at the top of the water column, while the light grey bars represent the levels of turbidity at the bottom. For the lowest concentration of turbidity (2.59 NTU), PAC only had a significant effect at the highest dosage of 16 mg Al/L, where the turbidity at the bottom increased to 50.7 NTU, as referred to in Table A.10 in the appendices. For an initial turbidity level of 6.3 NTU, PAC showed a significant effect at dosages of 8 and 16 mg/L. It can be observed from Figure 3.19 that, at a turbidity level of 13.3 NTU, PAC had an effect across all dosage levels. To better visualise these differences, Figures 3.17, 3.18, and Figure 3.19 were presented with separated y-axis scales in Figures A.2, A.3 and A.4 in the appendices. From Figure A.4, it becomes clearer that turbidity levels at the top decreased by less than half the initial value with the application of 1 mg/L of PAC. Variations in pH were similar for all initial turbidity levels, a decrease in pH due to increasing levels of PAC, with pH rapidly decreasing at concentration of 8 and 16 mg/L (min. pH 6.57). EC values did not vary significantly with PAC concentration and were more

dependent on the initial turbidity level.
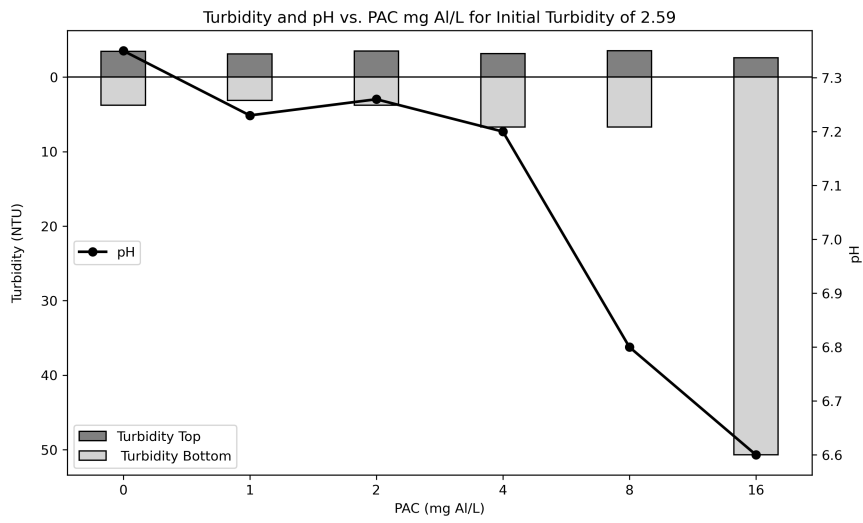
Figure 3.17: Turbidity values at the top (dark grey bars) and bottom (light grey bars) of the water column coupled with pH levels against varying concentrations of PAC in mg/L for an initial turbidity of 2.59 NTU.
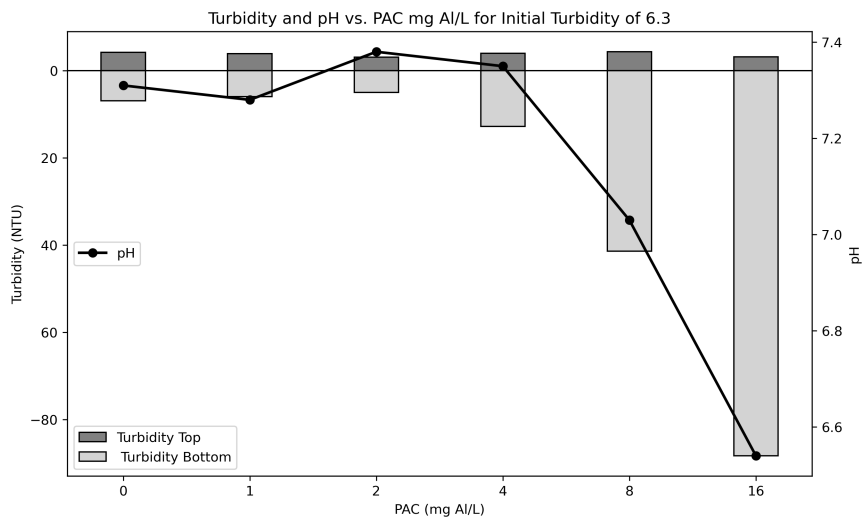
Figure 3.18: Turbidity values at the top (dark grey bars) and bottom (light grey bars) of the water column coupled with pH levels against varying concentrations of PAC in mg/L for an initial turbidity of 6.3 NTU.
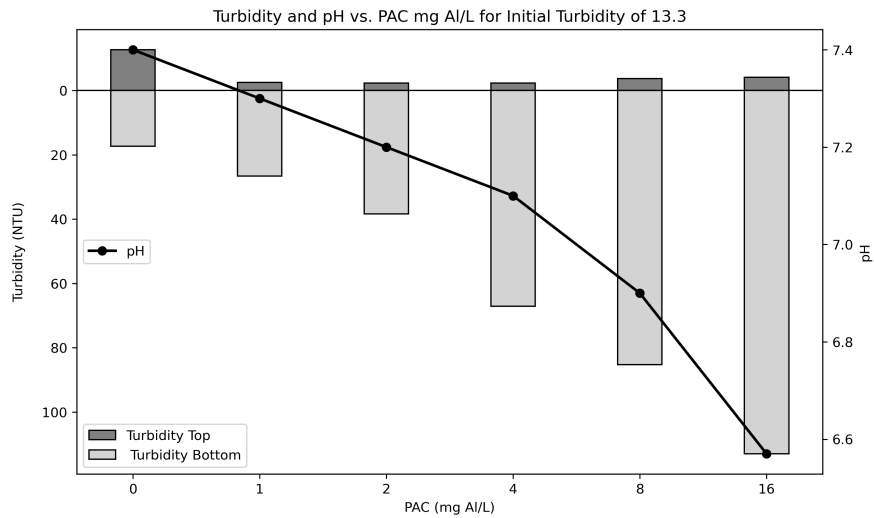
Figure 3.19: Turbidity values at the top (dark grey bars) and bottom (light grey bars) of the water column coupled with pH levels against varying concentrations of PAC in mg/L for an initial turbidity of 13.3 NTU.

3.4.2 Sediment

Water samples from cores with sediment treated with PAC (Cores C1 and C3) exhibited lower turbidity levels both during sediment resuspension (T1) and at the measured intervals of 15 and 30 minutes (T2 and T3), Table A.11. The average turbidity values for cores treated with PAC and those untreated followed the same trend; however, the treated cores consistently exhibited lower turbidity during and after sediment resuspension. Notably, the turbidity levels of the treated cores that were allowed to settle for 30 minutes post-resuspension approached the initial pre-treatment and pre-resuspension values. This trend is illustrated in Figure 3.20.
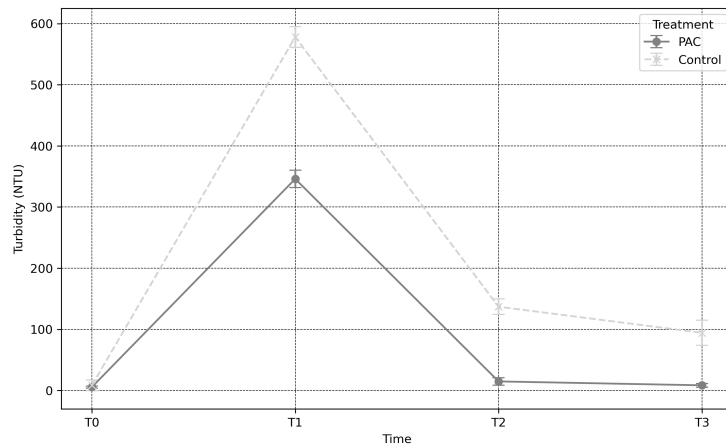
Figure 3.20: Changes in averaged turbidity levels over time in sediment treatment experiments with PAC and control samples at Location 1. Error bars indicate the variability in turbidity readings at specific time intervals post-treatment. T0 = pre-application of PAC, T1 = during resuspension event, T2 = after 15 minutes of resuspension event, T3 = 30 minutes after resuspension event.

Discussion

4.1 Water Quality

The results from November 2023 suggest that the lake experiences stratification, likely occurring during the spring and summer months, continuing until December. A clear stratification is observed beyond a depth of 11 meters, indicated by the presence of a thermocline and an oxicline [compare with mikes]. During this period, the lake's deeper layers see an increase in turbidity due to the absence of mixing in the water column. This condition of high turbidity could be exacerbated by resuspension events, leading to persistently high turbidity levels in the hypolimnion layer [17]. Further, the high nutrient levels observed at a depth of 14 meters point to active nutrient cycling within the lake, involving both the water column and the lake's sediment. In this environment, colder anoxic waters promote the release of phosphorus and ammonia. High nutrient levels from internal nutrient loads, combined with high light conditions during spring and summer, pose a risk that the lake becomes eutrophied, increasing water clarity problems. This potential for eutrophication is further exacerbated by the fact that warmer temperatures can enhance algal blooms, which may deplete oxygen in the water, leading to negative impacts on aquatic life and further degradation of water quality [33, 34]. During the winter, the profiles indicate a trend toward destratification, marked by more uniform temperature and oxygen saturation levels throughout the water column, indicative of seasonal mixing.

Possible external nutrient inputs to the lake could only be examined through one discharge pipe that was operational during the sampling event in December 2023. While water quality parameters from this sample show similar results to the surface water of Location 1, 2 and 3, it is important to point out that TN and TP concentration from the discharge pipe were around 3 to 0.5 times higher than that of the surface water from Location 1. Water quality parameters from surface water did not differ significantly across the three locations. Secchi disk measurements showed an average value 2.85 meters from the boat (2.7m min. and 3.10m max.) and an average of horizontal visibility 2.2 meters (min. 1.35 and 3.3 max.). These results are in agreement with results from the 2002 study "Duikers in de Mist" [17]. It can be difficult to correlate visibility to depth throughout the whole year as profiles of turbidity can form depending on the mixing stage of the lake [17]. A Secchi disk visibility of 3 meters generally indicates good water clarity and quality. This level of visibility suggests that the water is relatively clear, with lower concentrations of suspended solids and algae that could otherwise reduce light penetration and visibility [35]. Such conditions are often suitable for aquatic life. From a recreational point of view, specifically diving, this is very subjective and it is up to the Kaaiman divers to decide the desired visibility.

4.2 Lake Sediment and Resuspension

The results from the sediment core experiments provide evidence indicating that sediment plays a critical role in nutrient dynamics within the lake, particularly in relation to phosphorus (P) release from the sediment to the water column. This finding is further corroborated by the heightened concentrations of phosphorus observed in the deeper water layers during periods of lake stratification in Location 1 during the month of November, with P-PO_4 values in the lower water layer reaching 470.52 ug P/L. These findings imply a significant increase in P levels (TP and P-PO_4) in comparison to the study done on the lake in 2002 [17]. For example, the highest level of P-PO_4 measured was in July of 2002 (0.14 mg P/L), while the

23

current study found values of 0.47 mg P/L) in November 2023. Such periods of stratification typically see reduced water mixing, which allows nutrients from the sediment to accumulate in the lower water columns, subsequently influencing overall water quality and nutrient availability in the lake ecosystem [36]. The significant release of phosphorus from the sediment is especially pertinent considering its potential to fuel primary production [27]. During the summer months, when light penetration and temperatures are higher, the availability of these nutrients can lead to increased algal blooms and eutrophication. This underscores the sediment's role not only as a nutrient reservoir but also as a potential catalyst for ecological imbalance during warmer periods with potential negative effects to water clarity [14].

The physical characteristics of the sediment highlight the importance of resuspension in levels of turbidity and nutrient cycling, particularly at Location 1, where the top layer of the sediment has low density. This low density suggests a high susceptibility to resuspension, which could be easily triggered by disturbances such as those caused by fish movements or diving activities. Observations during sampling noted that the upper layers of the sediment were exceptionally fluffy, with more consolidated sediment only beginning at depths greater than 25-35 cm. This fluffy nature of the top sediment layers implies that even minimal physical disturbance could lead to significant resuspension, thus releasing more nutrients into the water column and potentially exacerbating turbidity and nutrient cycling issues [18].

The sediment's organic matter content was quantitatively assessed using Loss on Ignition (LOI) analysis, which measures the weight loss of sediment samples upon combustion at high temperatures. The high LOI values obtained for the top 5 cm of the sediment at Location 1 (19.90%) indicate a significant presence of organic material within the sediment layer. These high levels of organic matter correlate with enhanced phosphorus release, particularly noted under anoxic conditions prevalent in the deeper, stratified layers of the lake during warmer months [33]. Organic matter in aquatic systems, particularly when it decomposes, contributes significantly to the formation of humic acids, which can influence water turbidity. Humic acids are complex organic molecules that result from the decomposition of plant and animal residues, notably lignin and other biopolymers. Due to their large, aromatic structures, humic acids are highly reactive and inherently colored, often imparting a distinct brownish tint to the water [37]. This coloration decreases the transparency of the water, effectively increasing turbidity as less light penetrates through the water column. Humic acids can also form colloidal suspensions in water, which are fine enough to remain suspended in the water column for extended periods, thus directly contributing to increased turbidity. These colloids are stabilized by water chemistry variables such as pH and ionic strength, influencing their ability to remain in suspension. Consequently, the presence of high levels of organic matter, through the mediation of humic acids, can substantially affect the visual clarity and quality of aquatic environments by increasing turbidity and altering light dynamics within these ecosystems [37, 38].

4.3 Improving Water Clarity

Simply put, PAC clarifies water by causing suspended particles, which are not dense enough to settle by themselves, to coagulate and sink. A common reason for the low density of these suspended particles is their identical electrical charges, which lead to mutual repulsion and prevent aggregation. Consequently, they remain suspended in the water column. PAC, being a complex of polynuclear aluminum ions, possesses positively charged sites. These sites serve as a 'glue', with electrostatic forces between the positive charges of PAC and the negative charges of the suspended particles facilitating adhesion. Now bonded with PAC, the newly formed particles — referred to as flocs — gain sufficient mass to overcome buoyancy and settle at the bottom of the container. It is important to note that while PAC is effective at reducing water turbidity, the settled particles can be resuspended and an extra treatment step of filtration or dredging is applied [39].

The experiments conducted during this thesis demonstrated the potential for increasing water clarity by applying PAC to both the water column and sediment. When applied to water, PAC was more effective at higher turbidity levels and higher PAC concentrations. Even at the highest applied dosage of 16 mg P/L, water pH remained stable, avoiding the potential release of toxic aluminium species and staying within the ideal pH range (pH values under 6), [40]. At concentrations of 16 mg P/L, PAC reduced turbidity by up to 50% at a turbidity level of 6.33 NTU. This aligns with existing research indicating PAC's effectiveness across various aquatic environments [6, 8]. When applied directly to the sediment at a molar ratio of 10:1 PAC:P-PO$_4$, turbidity levels after 30 minutes of sediment resuspension returned to similar levels before

the suspension events. Direct application to the sediment shows potential advantages in binding more P, thereby reducing internal nutrient levels [32]. However, direct application to sediment introduces more complex application systems and thus comes at a higher financial cost [41].

The application of PAC as a standalone chemical treatment has shown to reduce turbidity and to reduce in lake nutrient cycling by binding itself to P-PO$_4$ species [40, 42]. Combined with a P-binding agent (e.g. lanthanum-modified bentonite), concentrations of 2 mg P/L of PAC were effective at reducing turbidity and settling cyanobacteria. This "Floc and Loc" method reduces not only suspended particles in the water column but also internal nutrient cycling in the lake [43, 44]. To further facilitate the rapid sedimentation of these particles, a ballast, such as sand or specialised clay, is added, called the "Floc and Sink" method. This addition increases the density of the formed flocs, causing them to sink more quickly to the bottom of the treatment basin This approach not only clarifies the water but also accelerates the process and decreases resuspension rates [45].

Future research on this front should focus on combining PAC with a P-binding agent or a ballast such as soil, which allows for lower concentrations of PAC to be applied with still effective results. Lower dosages of PAC reduce possible unwanted side effects such as decrease in pH which not only can diminish its effectiveness but also decrease water quality. The use of a P-binding agent and/or a ballast together with PAC can also have a longer effect in P binding compared to an application of PAC to the water column, especially considering how high resuspension rates activities can decrease the longevity of the effects of coagulants. A meta-analysis indicated that alum treatments improve water quality for an average of 21 years in deep lakes and 5.7 years in shallow ones, with disturbances from bottom-feeding fish like carp notably decreasing treatment effectiveness by stirring up sediment and releasing phosphorus [46, 47]. Diver induced resuspension might be enough to increase nutrient cycling and decrease the longevity of the application of a coagulant without the added positive effect of contributing to mixing of the stratified water layers as it happens in shallow lakes [46].

In considering the effectiveness of PAC, or another coagulant for that matter, in reducing sediment resuspension, it is essential to evaluate whether this reduction significantly enhances water clarity, particularly from the perspective of divers. The hypothesis is that applying PAC to either the sediment or the water column decreases resuspension rates. However, even with PAC treatment, some sediment resuspension will inevitably occur during diving activities close to the sediment layer. Therefore, the key question is whether the decrease in resuspension rates afforded by PAC is sufficient to maintain clear water conditions that do not negatively impact the visibility for divers during their underwater activities.

A successful restoration strategy for improving water clarity can involve a combination of chemical, physical, and biological measures [15]. A 'copy-paste' approach in measures should be avoided as it has led to the failure of most lake restoration attempts in the Netherlands over the long term [2]. For instance, should the use of PAC be deemed the appropriate solution for restoring Lake Berendonck, parameters from this study, such as PRP, provide a basis for calculating the amount of Al that can be utilised in the lake, depending on the chosen molar mass ratio [47, 48]. Another example is the underwater visibility measurements done by the divers can provide a more realistic optical quantity that translates more directly to underwater aesthetics and clarity than turbidity measurements alone [49].

Conclusion

Analysis of sediment and water samples indicates that internal nutrient release from the sediment can be a key driver of turbidity and nutrient levels in the lake which in turn affects overall water quality. Effective management of sediment could potentially reduce internal loading and recycling of nutrients, thereby improving water clarity and supporting aquatic life. Recognising the significance of sediment dynamics offers a pathway to mitigating issues of turbidity and nutrient enrichment, thus ensuring the health and sustainability of aquatic environments.

The results of our preliminary and limited experiments show that PAC, both applied to water and the sediment, can be a successful remediation strategy. When applied to the water column of the lake, PAC has the potential to effectively form flocs that settle, reducing turbidity. According to our experiments, this effect increases at concentrations above 8 mg/L and with waters that have turbidity levels of over 6 NTU. When applied directly to the sediment, PAC decreases sediment resuspension and increase the rate of sediment resettling. It's important to understand that while Poly Aluminium Chloride (PAC) helps in reducing resuspension and turbidity of sediments, it does not completely prevent these occurrences. If diving activities or other disturbances occur near the sediment layer, resuspension of sediments can still happen despite the presence of PAC. Further studies should be carried out on the applications of coagulants in combination with a ballast that has the potential to reduce turbidity even at low turbidity levels and decrease resuspension rates even further than a standalone coagulant.

I recommend that the Diving team Kaaiman continue taking visibility and turbidity measurements that will aid the researchers from the Aquatic Ecology and Water Quality Management, will help the diving team with making measurable goals related to the desired water clarity and in accessing a return on investment on possible remediation strategies. This study provided a foundation for the continuation of the project between the Kaaiman Diving Team and the WUR Science Shop. The study underscores the need for targeted sediment management strategies as part of lake restoration efforts and provides data that can guide a bespoke solution for the lake Berendonk. The analysis of water and sediment can be used as part of a larger comprehensive system analysis, the basis to choosing an remediation and intervention strategy.

Bibliography

1. Waajen, G. W. A. M., Faassen, E. J. & Lürling, M. Eutrophic urban ponds suffer from cyanobacterial blooms: Dutch examples. *Environment Science Pollution Research* **21,** 9983–9994 (2014).

2. Gulati, R. D. & van Donk, E. Lakes in the Netherlands, their origin, eutrophication and restoration: state-of-the-art review. *Hydrobiologia* **478,** 73–106 (2002).

3. Rosa Halbesma, T. *et al. Inzicht in kwaliteit van kleine wateren: Burgeronderzoek "Vang de Watermonsters" vult de blinde vlekken in ecologische waterkwaliteit op de kaart* Wetenschappelijke rapportage Projectnummer: 260-71009 (Nederlands Instituut voor Ecologie (NIOO-KNAW), Wageningen, Netherlands, 2023).

4. European Union. *The EU Environmental Implementation Review Country Report: The Netherlands* Staff Working Document SWD (2017) 52 final (European Commission, 2017). `https://ec.europa.eu/environment/eir/pdf/report_nl_en.pdf`.

5. Jayaweera, M. & Asaeda, T. Modeling of biomanipulation in shallow, eutrophic lakes: An application to Lake Bleiswijkse Zoom, the Netherlands. *Ecological Modelling* **85,** 113–127. ISSN: 0304-3800. `https://www.sciencedirect.com/science/article/pii/0304380094001537` (1996).

6. Lürling, M., Kang, L., Mucci, M., van Oosterhout, F., Noyma, N. P., *et al.* Coagulation and precipitation of cyanobacterial blooms. *Ecological Engineering* **158,** 106032. ISSN: 0925-8574. `https://www.sciencedirect.com/science/article/pii/S0925857420303207` (2020).

7. Sharpley, A. *et al.* Phosphorus legacy: overcoming the effects of past management practices to mitigate future water quality impairment. *Journal of Environmental Quality* **42,** 1308–1326 (2013).

8. Eleanor B. Mackay, S. C. M. *et al.* Geoengineering in lakes: welcome attraction or fatal distraction? *Inland Waters* **4,** 349–356 (2014).

9. Paerl, H. W. & Paul, V. J. Climate change: Links to global expansion of harmful cyanobacteria. *Water Research* **46.** Cyanobacteria: Impacts of climate change on occurrence, toxicity and water quality management, 1349–1363. ISSN: 0043-1354. `https://www.sciencedirect.com/science/article/pii/S0043135411004386` (2012).

10. Grobbelaar, J. in, 699–704 (Dec. 2009). ISBN: 9780123706263.

11. Smith, V., Tilman, G. & Nekola, J. Eutrophication: impacts of excess nutrient inputs on freshwater, marine, and terrestrial ecosystems. *Environmental Pollution* **100,** 179–196. ISSN: 0269-7491. `https://www.sciencedirect.com/science/article/pii/S0269749199000913` (1999).

12. Parma, S. The history of the eutrophication concept and the eutrophication in the Netherlands. *Hydrobiological Bulletin* **14,** 5–11. `https://doi.org/10.1007/BF02260267` (1980).

13. Edmondson, W. T., Anderson, G. C. & Peterson, D. R. Artificial Eutrophication of Lake Washington1. *Limnology and Oceanography* **1,** 47–53 (1956).

14. Stefanidis, K., Varlas, G., Papaioannou, G., Papadopoulos, A. & Dimitriou, E. Assessing temporal variability of lake turbidity and trophic state of European lakes using open data repositories. *Science of The Total Environment* **857,** 159618. ISSN: 0048-9697. `https://www.sciencedirect.com/science/article/pii/S0048969722067183` (2023).

15. Lürling, M. & Mucci, M. Mitigating eutrophication nuisance: in-lake measures are becoming inevitable in eutrophic waters in the Netherlands. *Hydrobiologia* (2020).

16. Stroom, J. & Kardinaal, W. How to combat cyanobacterial blooms: strategy toward preventive lake restoration and reactive control measures. *Aquatic Ecology* **50,** 541–576. `https://doi.org/10.1007/s10452-016-9593-0` (2016).

17. Van Hal, M. & Lürling, M. Divers in the fog: Scientific study on the degree of transparency around underwater house 'Aquavilla' in a deep diving pool. *Science Shop Wageningen Report* **195** (2004).

18. Niemistö, J., Holmroos, H. & Horppila, J. Water pH and sediment resuspension regulating internal phosphorus loading in a shallow lake – field experiment on diurnal variation. *Journal of Limnology* **70,** 3–10 (2011).

19. Søndergaard, M., Jensen, J. P. & Jeppesen, E. Role of sediment and internal loading of phosphorus in shallow lakes. *Hydrobiologia* **506–509,** 135–145 (2003).

20. Søndergaard, M., Kristensen, P. & Jeppesen, E. Phosphorus release from resuspended sediment in the shallow and wind-exposed Lake Arreso, Denmark. *Hydrobiologia* **228** (ed Golterman, H. L.) 91–99 (1992).

21. European Environment Agency (EEA). *Ecological status of surface water bodies* `https://www.eea.europa.eu/themes/water/european-waters/water-quality-and-water-assessment/water-assessments/ecological-status-of-surface-water-bodies`. Accessed: [06/11/2023]. 2018.

22. Huisman, J., Codd, G., Paerl, H., *et al.* Cyanobacterial blooms. *Nature Reviews Microbiology* **16,** 471–483. `https://doi.org/10.1038/s41579-018-0040-1` (2018).

23. Cooke, G., Welch, E., Peterson, S. & Nichols, S. *Restoration and Management of Lakes and Reservoirs* 3rd ed. `https://doi.org/10.1201/9781420032109` (CRC Press, 2005).

24. Nijman, T. P. *et al.* Phosphorus control and dredging decrease methane emissions from shallow lakes. *Science of The Total Environment* **847,** 157584. ISSN: 0048-9697. `https://www.sciencedirect.com/science/article/pii/S0048969722046824` (2022).

25. Salazar Torres, G., Silva, L., Rangel, L., *et al.* Cyanobacteria are controlled by omnivorous filter-feeding fish (Nile tilapia) in a tropical eutrophic reservoir. *Hydrobiologia* **765,** 115–129. `https://doi.org/10.1007/s10750-015-2406-y` (2016).

26. Meijer, M. L., de Boois, I., Scheffer, M., *et al.* Biomanipulation in shallow lakes in The Netherlands: an evaluation of 18 case studies. *Hydrobiologia* **408,** 13–30. `https://doi.org/10.1023/A:1017045518813` (1999).

27. Lürling, M. & van Oosterhout, F. Controlling eutrophication by combined bloom precipitation and sediment phosphorus inactivation. *Water Research* **47,** 6527–6537 (2013).

28. Immers, A. *et al.* Fighting internal phosphorus loading: An evaluation of the large scale application of gradual Fe-addition to a shallow peat lake. *Ecological Engineering* **83,** 78–89. ISSN: 0925-8574. `https://www.sciencedirect.com/science/article/pii/S0925857415300537` (2015).

29. *Onze Club - Kaaiman Dive Team* `https://www.kaaiman.nl/onze-club/`. Accessed: [insert date of access here]. 2023.

30. Larson, J., James, W., Fitzpatrick, F., *et al.* Phosphorus, nitrogen and dissolved organic carbon fluxes from sediments in freshwater rivermouths entering Green Bay (Lake Michigan; USA). *Biogeochemistry* **147,** 179–197 (2020).

31. Psenner R Pucsko R, S. M. Die Fraktionierung organischer und anorganischer Phosphorverbindungen von Sedimenten: Versuch einer Definition ökologisch wichtiger Fraktionen). *Hydrobiologie* **70,** 111–155 (1984).

32. De Vicente, I., Huang, P., Andersen, F. Ø. & Jensen, H. S. Phosphate Adsorption by Fresh and Aged Aluminum Hydroxide. Consequences for Lake Restoration. *Environ. Sci. Technol.* **42,** 6650–6655. `https://doi.org/10.1021/es800053s` (2008).

33. Jeong, Y.-H., Choi, Y.-H. & Kwak, D.-H. Effect of Benthic Flux on the Nutrient Dynamics of Bottom Water during Stratification in an Artificial Brackish Lake. *Water* **16,** 958 (2024).

34. Essington, T. E. & Carpenter, S. R. Nutrient Cycling in Lakes and Streams: Insights from a Comparative Analysis. *Ecosystems* **3,** 131–143 (2000).

35. Zhang, L. *et al.* Turbidity dynamics of large lakes and reservoirs in northeastern China in response to natural factors and human activities. *Journal of Cleaner Production* **368,** 133148. ISSN: 0959-6526. https://www.sciencedirect.com/science/article/pii/S0959652622027378 (2022).

36. Mucci, M. N. *From Green to Transparent Waters: Managing Eutrophication and Cyanobacterial Blooms by Geo-Engineering* PhD thesis (Wageningen University, Wageningen, The Netherlands, 2019). ISBN: 978-94-6343-441-6.

37. Steinberg, C. E. W. *Ecology of Humic Substances in Freshwaters: Determinants from Geochemistry to Ecological Niches* (Springer-Verlag, Berlin, Heidelberg, 2003).

38. Thurman, E. M. *Organic Geochemistry of Natural Waters* (Martinus Nijhoff/Dr W. Junk Publishers, Dordrecht, 1985).

39. Bratby, J. Coagulation and Flocculation in Water and Wastewater Treatment - Second Edition. *Water Intelligence Online* **5,** 31–41 (Oct. 2006).

40. Reitzel, K., Hansen, J., Andersen, F. Ø., Hansen, K. S. & Jensen, H. S. Lake Restoration by Dosing Aluminum Relative to Mobile Phosphorus in the Sediment. *Environmental Science & Technology* **39.** PMID: 15984792, 4134–4140 (2005).

41. Schütz, J., Rydin, E. & Huser, B. J. A Newly Developed Injection Method for Aluminum Treatment in Eutrophic Lakes: Effects on Water Quality and Phosphorus Binding Efficiency. *Lake and Reservoir Management* **33,** 152–162. https://www.tandfonline.com/doi/full/10.1080/10402381.2017.1318418 (2017).

42. Waajen, G., van Oosterhout, F., Douglas, G. & Lürling, M. Management of Eutrophication in Lake De Kuil (The Netherlands) Using Combined Flocculant – Lanthanum Modified Bentonite Treatment. *Water Research* **97,** 83–95. https://www.elsevier.com/locate/watres (2016).

43. De Magalhães, L., Noyma, N., Furtado, L. & et al. Managing Eutrophication in a Tropical Brackish Water Lagoon: Testing Lanthanum-Modified Clay and Coagulant for Internal Load Reduction and Cyanobacteria Bloom Removal. *Estuaries and Coasts* **42,** 390–402. https://doi.org/10.1007/s12237-018-0474-8 (2019).

44. Waajen, G., van Oosterhout, F., Douglas, G. & Lürling, M. Geo-engineering experiments in two urban ponds to control eutrophication. *Water Research* **97.** Special Issue on Geo-engineering to Manage Eutrophication in Lakes, 69–82. ISSN: 0043-1354. https://www.sciencedirect.com/science/article/pii/S0043135415303961 (2016).

45. Qasim, M., Park, S., Moon, Y. & Kim, J.-O. Developing a model to determine the settling velocity of ballasted flocs. *Journal of Environmental Chemical Engineering.* Available online 21 September 2020 (2020).

46. White, M., Gaffney, S., Bowers, D. & Bowyer, P. Interannual Variability in Irish Sea Turbidity and Relation to Wind Strength. *Biology and Environment: Proceedings of the Royal Irish Academy* **108,** 83–90 (2003).

47. Huser, B. J. *et al.* Longevity and effectiveness of aluminum addition to reduce sediment phosphorus release and restore lake water quality. *Water Research* **97,** 122–132. ISSN: 0043-1354. https://www.sciencedirect.com/science/article/pii/S0043135415301020 (2016).

48. Lewandowski, J., Schauser, I. & Hupfer, M. Long term effects of phosphorus precipitations with alum in hypereutrophic Lake Süsser See (Germany). *Water Research* **37,** 3194–3204. ISSN: 0043-1354. https://www.sciencedirect.com/science/article/pii/S0043135403001374 (2003).

49. Davies-Colley, R. J. & Smith, D. G. Turbidity, Suspended Sediment, and Water Clarity: A Review. *Journal of the American Water Resources Association* **37,** 1085–1101 (2001).

Appendices

A.1   Protocol for Visibility

This protocol outlines a standardised procedure for divers, combining the use of the Secchi disk with the collection of water samples for turbidity measurements. The Secchi disk, a simple yet powerful tool, consists of a round, black and white disc that is submerged in water until its contrasting quadrants become imperceptible to the human eye, providing an assessment of water visibility. Along with these visibility measurements, divers are instructed to collect water samples, enhancing the protocol's utility in monitoring aquatic environments. The specifics of turbidity measurement using a turbidimeter are covered in a separate document. By adhering to these methods, divers can contribute valuable data, essential for informed decision-making regarding the aquatic environment's condition.

Measuring Horizontal and Vertical Visibility

Accurate measurement of water visibility using the Secchi disk is a static process but varies depending on several environmental and human factors. For example, experienced divers might disturb the water less compared to novices, which could affect the visibility. Therefore, it is essential to conduct these measurements under a variety of conditions and by divers of different skill levels. So please try to vary the factors as much as possible within the reality of the diving activities. Such diverse data collection helps in creating a more accurate and reliable assessment of the aquatic environment.

Procedure

Materials Needed:

1. Secchi disk - Essential for visibility measurement.

2. Rope or line - Marked for depth and distance measurements.

3. Buoy or float - To mark the surface location and for stability.

4. Diving equipment - Includes wetsuit, fins, mask, snorkel, and SCUBA gear.

5. Writing pad and pen - Waterproof, for recording measurements underwater.

6. Dive computer - To monitor depth, time, and decompression status.

7. Underwater flashlight - For enhanced visibility in low-light conditions.

8. Dive flag - To indicate divers are in the water for surface-level safety.

9. First-aid kit - For handling minor injuries or emergencies.

10. Emergency signalling device - Such as a whistle or surface marker buoy for safety.

11. Water sample containers

12. Labels and waterproof markers - To label each sample with depth, location, and time of collection.

Preparation

1. Gather all necessary materials: Secchi disk, marked rope or line, buoy or float, diving equipment, waterproof writing pad and pen, dive computer, underwater flashlight, dive flag, first-aid kit, emergency signalling device, water sample containers, labels, waterproof markers, and gloves.

2. Attach the Secchi disk securely to the rope or line, ensuring it is centered and hangs horizontally. Check that the markings on the rope or line are clearly visible.

3. Inspect your diving equipment thoroughly, ensuring everything is in optimal working condition. This includes checking your wetsuit, fins, mask, snorkel, SCUBA gear, and dive computer.

4. Pre-label the water sample containers with relevant details such as date, location, and depth for efficient and organised sample collection.

5. Test the functionality of your underwater flashlight, especially if you anticipate low-light conditions.

6. Select the specific location in the lake where visibility measurements and water sample collection will be conducted. The location can be determined by the profile of the lake in the Annex of this document. The location can be in the Red, Yellow, Green or Blue zone (refer to the profile of the lake in the Annex). Remember that after the measurement, you will need to point out the location in the zone that the measurement took place.

7. Review the dive plan, including entry and exit points, dive path, communication signals, and procedures for sample collection. Ensure that all divers are familiar with the plan and safety procedures.

8. Set up the dive flag to alert nearby boats or other watercraft to the presence of divers.

9. Ensure that a designated person on the surface is informed of your dive plan, expected return time, and sample collection activities.

Vertical Visibility and Water Collection

1. Dive to the desired depth where visibility is to be measured. Ensure that you are at a stable position.

2. Begin to slowly lower the Secchi disk into the water vertically from your position, ensuring it descends in a straight line. This can be done at various depths, just at the surface.

3. Continue lowering the disk steadily. Observe carefully and mark the point on the rope or line when the Secchi disk first becomes invisible due to water opacity.

4. After marking this first point, start raising the disk slowly. e the point on the rope or line when the disk becomes visible again.

5. Calculate the average of the two depths (when the disk disappeared and reappeared) to determine the vertical visibility at that depth and record the measurement. Mark the level of the diver on a scale of 1 to 5.

6. After recording the vertical visibility, collect a water sample at the starting depth. Ensure proper handling to avoid contamination.

7. Securely seal the water sample container and label it with the depth, location, and time of collection.

8. Perform routine diving activities around the same location and repeat the procedure for vertical visibility and water collection at different depths as needed.

9. In case of resuspension occurring before the first measurement (prior to initiating diver activity), e it down in the observations part of this protocol.

10. Make sure to e down all of the information needed regarding the measurement in the table included in this protocol. Also mark the location of the measurement in the image of the profile of the lake with the date of the measurement. You can extend an arrow from the marking of the location and write down the date.

Horizontal Visibility

1. Diver and assisting diver must be at the same depth, ensuring they are comfortably stable and the water around them is undisturbed.

2. Diver A holds the Secchi disk at arm's length. The disk should be fully extended and perpendicular to the line of sight towards Diver B.

3. Diver B, holding one end of a marked rope or line, begins to move horizontally away from Diver A. The movement should be slow and steady to maintain a consistent depth and alignment.

4. Diver B continues moving away until the Secchi disk is no longer visible. At this moment, Diver B should stop and mark or record the distance on the rope or line. This distance represents the point of disappearance.

5. Diver B then carefully moves back towards Diver A until the Secchi disk becomes visible again. Record the distance at the point of reappearance.

6. Calculate the average of the two distances (disappearance and reappearance) to determine the horizontal visibility at that location and record the measurement. Record the depth that the horizontal visibility measurement was done. Mark the level of the diver on a scale of 1 to 5.

7. Perform routine diving activities around the same location and repeat the procedure for horizontal visibility.

8. In case of resuspension occurring before the first measurement (prior to initiating diver activity), e it down in the observations part of this protocol. Make sure to e down all of the information needed regarding the measurement in the table included in this protocol. Also mark the location of the measurement in the image of the profile of the lake with the date of the measurement. You can extend an arrow from the marking of the location and write down the date.

Safety Measures

Prioritize safety in all underwater activities. Adhere to guidelines from diving authorities, ensure equipment is well-maintained, and practice effective communication. Dive in pairs, plan each dive, stay aware of surroundings and potential risks, and follow depth and ascent protocols to avoid diving complications. Document each dive, be prepared for emergencies, and ensure a surface contact is informed of your activities.

A.2 Depth Profile of the Diving Lake
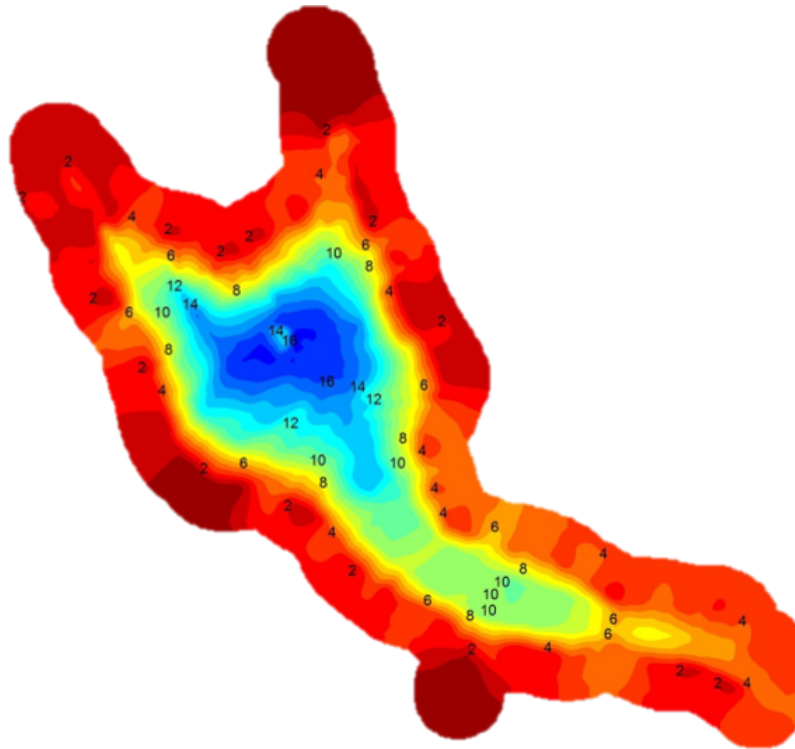
Figure A.1: Depth profile of the lake using sonar measurements provided by the fisherman association: Hengelsportvereniging De Sportvisser.

—

A.3   Psenner Methodology

Date: modified 2015/2019 (ML/WB) update: dec. 2022 (WB)

Reference: Modified by Miguel Lurling from Paludan & Jensen 1995, Wetlands 15 365-373 Sequential Extraction of Phosphorus in Freshwater Wetland and Lake sediments: significance of Humic Acids.

Shaking

1. Use shaker <140 rpm

2. Shake tubes horizontally

Centrifugation

1. 5 minutes at 5000 rpm

Filtration

- 1,2 μm (GF/C)filter, vacuum filtration

First phase: Oxygen-free nanopure water $\rightarrow$ It aims to release the available P, which is adsorbed mostly on iron/manganese oxides at Fe and $CaCO_3$ sites.

1. Add 25 mL of oxygen-free nanopure water.

2. Replace air with N_2 and close tube.

3. Shake tubes for 30 minutes on shaker.

4. Place the tubes in centrifuge, centrifuge.

5. Decant supernatant carefully into labelled 100 mL PE bottle, save pellet.

6. Repeat extraction with 25 mL oxygen-free water for 5 minutes and centrifuge.

7. Decant and combine supernatant.

8. Filter the supernatant over a GF/C filter and collect 30 mL filtrate in a labelled 50 mL PE bottle.

9. Store in the freezer

10. Measure PO4-P

Second Phase: BD-reagent (bicarbonate-dithionite mixture) $\rightarrow$ Aim: stronger reductant that will release the SRP bound mainly to Fe-hydroxides and Mn-compounds.

1. Add 25 mL BD-reagent, oxygen-free, to sediment pellet and close tube.

2. Shake tubes for 30 minutes.

3. Replace air with N_2 and close tube.

4. Centrifuge.

5. Decant supernatant into 100 mL PE bottles.

6. Add 25 mL BD to pellet, replace air with N_2.

7. Shake tubes on shaker for 5 minutes.

8. Centrifuge.

9. Decant and combine supernatant. Save pellet.

10. Put sample bottles in aeration-set-up.

11. Aerate for 30 minutes (removal of dithionite; keeps Fe and PO_4 in solution).

12. Add 3 mL 2M H_2SO_4 to the combined supernatants and mix.

13. Filter combined supernatants, collect 30 mL filtrate into 50 mL PE bottle. Label and store at 4 °C.

14. Measure PO4-P and TP (total fraction of the dissolved).

Third Phase: Sodium Hydroxide (NaOH) → It will extract SRP sorbed by clay- and metal-oxides (Al) at pH > 10.

1. Add 25 mL 0,1 M NaOH to the sediment pellet and close tube.

2. Shake tubes for 30 minutes on shaker.

3. Centrifuge and check pH, if pH > 10 add extra 1 M NaOH till pH is > 10 (ask technician).

4. Decant supernatant into 100 mL PE bottle.

5. Add 25 mL NaOH to sediment pellet.

6. Shake again 30 minutes on shaker and centrifuge.

7. Combine supernatants into 100 mL PE bottle.

8. Add 25 mL of milli-Q water to the sediment and shake for 5 minutes, centrifuge.

9. Decant the third supernatant in the same 100 mL PE bottle.

10. Add 1.5 mL of 2 M H_2SO_4 in the supernatant and mix.

11. Filter the supernatant and collect 30 mL filtrate into 50 mL bottle.

12. Measure PO4-P and TP (total fraction of the dissolved).

Fourth Phase: Hydrochloric acid → Aim to release P bound to carbonates and residual P. This is hardly available.

- Add 25 mL 0.5 M HCl and close tube. Shake for 1 hour

- Centrifuge

- Decant supernatant into 100 mL PE bottle

- Add 25 mL Milli-Q water to the sediment, shake for 5 minutes.

- Centrifuge

- Combine supernatants and filter through GF/C. collect 30 mL filtrate and store at 4°C.

- Save pellet

- Measure PO4-P and TP (total fraction of the dissolved).

Fifth Phase: Finally, the sediment pellet will be extracted using stronger acid and higher temperature. This will give the refractory P.

1. Move the pellet to crucibles using little milli-Q water.

2. Dry crucibles at 105 °C in drying oven, over-night.

3. Ignite pellet at 550 °C for 2 hours.

4. Cool down and "crumble" pellet in crucible.

5. Add 10 mL 2M H_2SO_4 and mix.

6. Place crucibles with lid on hot-plate (in fume hood) and boil 10 minutes at 150 °C.

7. Take-up sample by 10 mL syringe, add filter-disc.

8. Filter sample in a labelled 15 mL tube.

9. Measure TP.

Measure PO4-P and TP (total fraction of the dissolved).

A.4   Data - Water Analysis

Table A.1: Field and laboratory measurements of the lake water collected on 23.11.2023. The Secchi disk measurement was 2.75 meters during a cloudy day. TSS = Total suspended Solids, VSS = Volatile Suspended Solids, chl-a = Chlorophyll-a.

Location	Depth	O_2 (mg/L)	O_2 %	T (°C)	pH	EC (uS/cm)	Turbidity (NTU)	TSS ug/L	VSS ug/L	chla-a (ug/L)
1	0	5.2	46.4	10.3	6.6	382	1.34	1.00	0.69	1.94
1	2	5.15	46	10.2	6.85	380	1.51	1.50	0.93	1.6
1	4	5.1	45.5	10.1	6.93	380	1.5	1.08	0.17	1.62
1	6	5.05	45.1	10.1	6.95	380	2.51	0.75	0.67	1.59
1	8	5.02	44.9	10.1	7,0	381	1.83	0.50	0.30	1.61
1	10	4.9	43.8	10.1	7.1	380	1.98	0.70	0.40	1.51
1	11	0.3	2.5	7.5	7.16	384	2.09	0.30	0.30	1.43
1	12	0.38	3	9.1	7.16	401	5.28	0.40	0.00	2.05
1	14	0.22	1.8	6.7	7.17	414	18.78	0.50	0.17	4.43
1	16	n/a	n/a	n/a	7.15	428	36.3	0.33	0.00	5.21
2	0	5.39	48.5	10.4	7.22	380	2.3	1.40	0.40	4.93
3	0	4.98	45.7	10.4	7.31	378	0.9	0.43	0.71	0.37

Table A.2: Field and laboratory measurements of the lake water collected on 12.12.2023. The Secchi disk measurement was 2.70 meters during a sunny day. TSS = Total suspended Solids, VSS = Volatile Suspended Solids, chl-a = Chlorophyll-a.

Location	Depth	O_2 (mg/L)	O_2 %	T (°C)	pH	EC (uS/cm)	Turbidity (NTU)	TSS ug/L	VSS ug/L	chla-a (ug/L)
1	0	5.03	42.5	7.1	7.45	384	1.18	0.37	0.12	1.99
1	2	4.88	41	6.9	7.55	388	1.58	0.49	0.24	1.59
1	4	4.82	40.4	6.9	7.59	389	1.58	14.25	14.13	1.53
1	6	4.75	39.9	6.9	7.58	388	1.98	0.48	0.36	1.67
1	8	4.13	34.5	6.7	7.59	390	1.46	0.50	0.37	1.45
1	10	3.89	32.5	6.7	7.57	390	1.97	0.71	0.43	1.54
1	11	3.75	31.3	6.7	7.54	390	1.87	0.37	0.12	1.53
1	12	3.56	29.7	6.6	7.58	392	2.88	0.00	0.27	1.58
1	14	3	25	6.6	7.54	390	2.06	0.61	0.61	1.67
1	16	n/a	n/a	n/a	7.52	406	180.4	2299	11780	0
2	0	4.62	39	7.4	7.53	390	1.54	0.49	0.37	1.5
3	0	3.88	31.6	7.5	7.53	391	1.65	0.62	0.74	1.64

Table A.3: Field and laboratory measurements of the lake water collected on 25.01.2023. The Secchi disk measurement was 3.10 meters during a sunny day. TSS = Total suspended Solids, VSS = Volatile Suspended Solids, chl-a = Chlorophyll-a.

Location	Depth	O_2 (mg/L)	O_2 %	T (°C)	pH	EC (uS/cm)	Turbidity (NTU)	TSS ug/L	VSS ug/L	chla-a (ug/L)
1	0	8.15	63.4	5	7.44	390	1.68	0.68	0.23	2.07
1	2	8.06	62.6	4.8	7.53	392	2.69	0.93	0.17	2.11
1	4	8.05	62.3	4.8	7.57	389	3.53	0.71	0.29	2.01
1	6	8.03	62.1	4.8	7.6	389	5.59	0.58	0.09	2.19
1	8	7.99	61.8	4.8	7.62	391	2.5	0.47	0.16	2.33
1	10	7.94	61.3	4.7	7.63	392	1.66	0.65	0.28	2.28
1	11	7.85	60.7	4.7	7.61	390	3.13	0.23	0.07	2.34
1	12	7.82	60.3	4.7	7.6	389	2.05	0.47	0.73	1.93
1	14	7.56	58.3	4.6	7.55	391	1.95	0.51	0.10	1.81
1	16	7.46	57.4	4.6	7.45	392	2.08	0.69	0.07	0
2	0	7.89	63.6	4.8	7.5	393	2.12	0.97	1.67	2.64
3	0	7.99	63.8	4.9	7.78	373	0.85	0.56	0.00	2.3

Table A.4: **Nutrient levels from water samples collected on the 23/11/2023**: Concentrations of total nitrogen, ammonia, nitric nitrate, ortho phosphate, and total phosphate measured at various depths across the three distinct sampling locations. The data exemplifies the variability in nutrient levels within the water column.

Location	Depth (m)	Total Nitrogen (mg N/L)	Ammonia (mg N/L)	Nitrite Nitrate (mg N/L)	Ortho Phosphate (ug P/L)	Total Phospate (mg P/L)
1	0	0.64	0.12	0.06	33.73	0.04
1	2	0.66	0.17	0.05	13.98	0.03
1	4	0.63	0.17	0.06	15.81	0.03
1	6	0.64	0.19	0.06	24	0.03
1	8	0.72	0.19	0.05	14.95	0.03
1	10	0.62	0.19	0.06	15.31	0.02
1	11	0.3	0.21	0.05	34.8	0.03
1	12	0.5	0.51	0.02	127.85	0.13
1	14	1.13	1.2	0.01	470.52	0.44
1	16	1.86	1.28	0.01	422.76	0.48
2	0	0.42	0.11	0.08	5.4	0.04
3	0	0.15	0.21	0.05	50.04	0.01

Table A.5: **Nutrient levels from water samples collected on the 12/12/2023**: Concentrations of total nitrogen, ammonia, nitric nitrate, ortho phosphate, and total phosphate measured at various depths across the three distinct sampling locations. The data exemplifies the variability in nutrient levels within the water column.

Location	Depth (m)	Total Nitrogen (mg N/L)	Ammonia (mg N/L)	Nitrite Nitrate (mg N/L)	Ortho Phosphate (ug P/L)	Total Phospate (mg P/L)
1	0	0.27	0.25	0.13	49.52	0.04
1	2	0.47	0.17	0.18	74.05	0.05
1	4	0.44	0.12	0.21	44.96	0.04
1	6	0.51	0.21	0.2	42.69	0.04
1	8	0.53	0.13	0.18	44.31	0.04
1	10	0.55	0.19	0.23	60.8	0.05
1	11	0.56	0.15	0.24	45.47	0.05
1	12	0.7	0.09	0.28	50.51	0.04
1	14	0.84	0.17	0.23	41.63	0.05
1	16	2.43	1.07	0.01	6.68	0.04
2	0	1.05	0.17	0.21	33.47	0.04
3	0	0.85	0.09	0.2	27.37	0.02
4	0	0.93	0.11	0.26	57.88	0.06

Table A.6: **Nutrient levels from water samples collected on the 25/01/2024**: Concentrations of total nitrogen, ammonia, nitric nitrate, ortho phosphate, and total phosphate measured at various depths across the three distinct sampling locations. The data exemplifies the variability in nutrient levels within the water column.

Location	Depth (m)	Total Nitrogen (mg N/L)	Ammonia (mg N/L)	Nitrite Nitrate (mg N/L)	Ortho Phosphate (ug P/L)	Total Phospate (mg P/L)
1	0	0.9	0.05	0.49	23.8	0.04
1	2	0.93	0.05	0.5	20.29	0.02
1	4	0.69	0.04	0.48	24.19	0.02
1	6	0.61	0.06	0.1	7.4	0.01
1	8	0.83	0.06	0.51	25.6	0.03
1	10	0.76	0.06	0.5	27.71	0.03
1	11	0.88	0.08	0.49	27.63	0.03
1	12	0.94	0.03	0.45	27.6	0.03
1	14	0.91	0.08	0.5	34.69	0.03
1	16	0.95	0.13	0.5	27.58	0.03
2	0	0.84	0.09	0.51	20.57	0.02
3	0	0.55	0.1	0.24	6.33	0.01

Parameter	F-value	p-value
O2 (mg/L)	0.058	0.944
O2%	0.073	0.930
Temperature (°C)	0.0018	0.998
pH	0.293	0.756
EC (uS/cm)	0.0078	0.992
Turbidity (NTU)	1.433	0.310
TSS	1.110	0.389
VSS	4.231	0.071
Chlorophyll-a	1.528	0.291

Table A.7: F-value and P-value from the ANOVA results for water quality parameters across different locations.

A.5   Data - Sediment Analysis

Table A.8: Loss on drying (LOD %), loss on ignition (LOI %), and density (g/mL) measurements for each fraction of sediment samples from locations 1, 2, and 3.

Location	Fraction (cm)	LOD (%)	LOI (%)	Density (g/mL)
1	0 - 5	90.27	19.90	1.06
1	5 - 10	86.30	16.77	1.03
1	10 - 20	64.10	7.05	1.21
2	0 - 5	82.88	17.23	1.14
2	5 - 10	81.06	18.44	1.09
2	10 - 20	76.64	15.21	1.22
3	0 - 5	74.06	9.28	1.13
3	5 - 10	68.24	7.88	1.14
3	10 - 20	52.32	5.10	1.21

Table A.9: Concentration of Refractory P and PRP phases (mg/g sediment) at different sediment depths across three locations.

Fraction	0-5 cm	5-10 cm	10-20 cm
LOC1			
Refractory P	1.687	1.207	0.487
PRP	2.803	2.822	0.668
LOC2			
Refractory P	0.994	0.928	0.845
PRP	0.916	0.811	0.516
LOC3			
Refractory P	0.784	0.589	0.403
PRP	0.510	0.440	0.282

A.6 Data - Coagulant Experiment
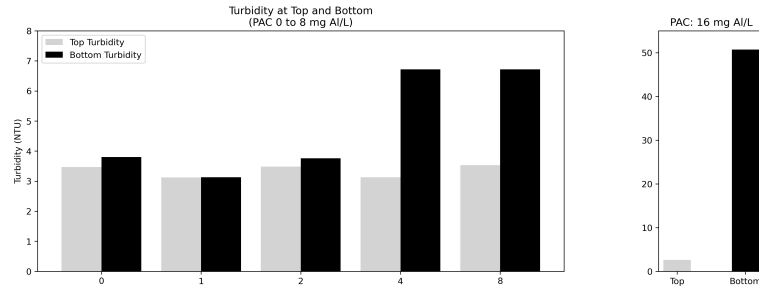
Figure A.2: Comparison of turbidity levels at the top (in dark grey) and bottom (in black) of the water column at varying dosages of PAC (0, 1, 2, 4 and 8 mg/L for the left graph and 16 mg/L for the right graph) for an initial turbidity of 2.59 NTU.
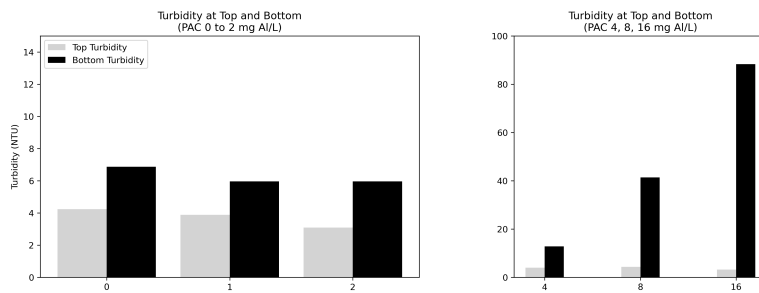
Figure A.3: Comparison of turbidity levels at the top (in dark grey) and bottom (in black) of the water column at varying dosages of PAC (0, 1, 2 mg/L for the left graph and 4, 8, 16 mg/L for the right graph) for an initial turbidity of 2.59 NTU.
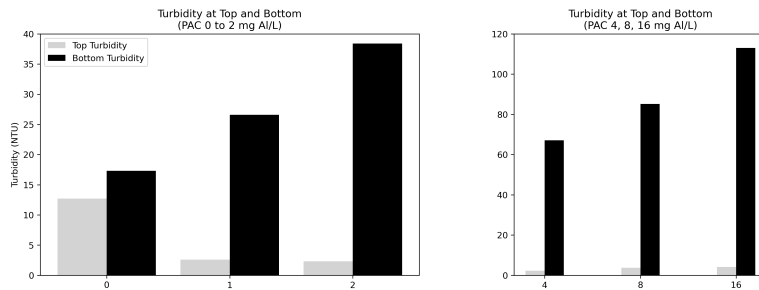
Figure A.4: Comparison of turbidity levels at the top (in dark grey) and bottom (in black) of the water column at varying dosages of PAC (0, 1, 2 mg/L for the left graph and 4, 8, 16 mg/L for the right graph) for an initial turbidity of 2.59 NTU.

Table A.10: Values of turbidity measured at the top and the bottom of the water column for initial turbidity values of 2.59, 6.3, and 13.3 NTU after the application of PAC in five different concentrations. pH and EC were measured after the application of PAC.

Ini. Turbidity (NTU)	PAC mg/L	Samplie Location	Turbidity (NTU)	EC (uS/cm)	pH	Ini. Turbidity (NTU)	PAC mg/L	Samplie Location	Turbidity (NTU)	EC (uS/cm)	pH	Ini. Turbidity (NTU)	PAC mg/L	Samplie Location	Turbidity (NTU)	EC (uS/cm)	pH
2.59	0	T	3.47	394	7.35	6.3	0	T	4.23	344	7.31	13.3	0	T	12.7	368	7.4
2.59	0	B	3.8			6.3	0	B	6.87			13.3	0	B	17.3		
2.59	1	T	3.12	335	7.23	6.3	1	T	3.88	354	7.28	13.3	1	T	2.58	410	7.3
2.59	1	B	3.13			6.3	1	B	5.96			13.3	1	B	26.6		
2.59	2	T	3.48	336	7.26	6.3	2	T	3.09	360	7.38	13.3	2	T	2.3	413	7.2
2.59	2	B	3.76			6.3	2	B	4.96			13.3	2	B	38.4		
2.59	4	T	3.13	384	7.2	6.3	4	T	4.01	364	7.35	13.3	4	T	2.3	416	7.1
2.59	4	B	6.72			6.3	4	B	12.8			13.3	4	B	67.1		
2.59	8	T	3.53	386	6.8	6.3	8	T	4.33	365	7.03	13.3	8	T	3.74	418	6.9
2.59	8	B	6.72			6.3	8	B	41.4			13.3	8	B	85.2		
2.59	16	T	2.61	390	6.6	6.3	16	T	3.17	367	6.54	13.3	16	T	4.13	413	6.57
2.59	16	B	50.7			6.3	16	B	88.3			13.3	16	B	113		

Table A.11: Levels of turbidity for for PAC applied to the sediment of fours cores from location 1, and controls, across time intervals. T0: Before resuspension or application of PAC, T1: During resuspension after the application of PAC, T2: After 15 minutes of resuspension event, T3: After 30 minutes of resuspension event.

Core	Treatment	Turb. (NTU) - T0	Turb. (NTU) - T1	Turb. (NTU) - T2	Turb. (NTU) - T3
C1	PAC	6.7	356	10.4	6.42
C3	PAC	4.5	336	19.3	10.6
C2	Control	2.18	590	146	79.8
C5	Control	14.7	566	128	109